Master Final Thesis

Energy Engineering - Renewable

Comparison Study of Geothermal Power Generating Technologies for Kepahiang Reserve in Sumatra, Indonesia

REPORT

Author: Angelina V. Kalianda
Director: Professor J.J. Felipe
Centre tutor: Professor Enrique Velo

Presentation: February 2017

ETSEIB

Escola Tècnica Superior
d'Enginyeria Industrial de Barcelona

Review

Indonesia is urgently calling to improve their electrification rate as basic human need, adding to its already growing demand for more. This call cannot be ignore given that Indonesia is the fourth most populous country and one of the biggest carbon emitters in the world despite that it is also rich of clean natural resources such as geothermal and hydropower. Yet, the government faces many challenges to reach its goal of providing access to electricity without adding to the carbon footprint. Global community is inclined to take notice and help.

This study is to assist the government to develop its abundant geothermal reserves by comparing three different geothermal technologies for the specific reserve site of Kepahiang in Sumatra Indonesia. The site produces high temperature geofluid at 250°C from volcanic system. Still, the acidic nature of the geofluid forces us to look at different alternatives not only the obvious solution of flash cycle plant technology for high temperature system. Three systems are considered: double-flash plant, binary plant, and hybrid single flash with binary bottoming unit.

The result points to hybrid flash/binary system as possibly the best solution for Kepahiang reserve out of the three options.

Summary

1. Introduction

1.1. Background

Indonesia, as an archipelagic nation, comprises 17,508 islands spanning over 5,000 km and from east to west, 1,700 km from north to south, and over 1,900,000 square kilometers of land. It makes the world's fifteenth largest and fourth most populous country with approximately 258 million habitants in 2015[1]. With average economy growth rate of 5.7% between 2000 and 2012, it is the largest in Southeast Asia and the sixteenth largest globally. Indonesian government strives to make Indonesia to be the top-ten economies globally. Indonesia is also a member of G20. [1]

Despite all, Indonesia has only achieved 84% electrification ratio by the end of 2014, lowest in the region [2].

Country	Electrification rate[1]	Electricity Consumption (kWh per capita)[2]
Indonesia	84.3%*	0.7
Philippines	89.7%	0.6
Vietnam	97.3%	1.1
Thailand	99.3%	2.3
Malaysia	99.4%	4.2
Singapore	100%	8.4

*figure for 2014

Source: 1 PLN, ASEAN-RESP 2012; 2 World Bank

Fig. 1.1 Southeast Asia electrification rate of 2014. [3]

Electrification rate has been linked to Human Development Index (HDI). Countries with better access to electricity achieve higher HDI levels since facilitation of basic needs, such health services, educational institutions, and economic activities, is improved. Government aims to achieve 99.4% of electrification rate by 2024 and 115 GW installed generation capacity by 2025, which requires electric generation growth of 7 GW/year [1] [3].

The urgent need to increase the electric generation capacity is more than ever now with the rising demand approximately 8.1% per year for the last 5 years, mostly from the residential sector. Thus far, the demand has not been match with the addition of the capacity that only

[1] United Nations: Population Division, Data Query. https://esa.un.org/unpd/wpp/DataQuery/ (2017)

[2] http://kepahiangkab.go.id/index.php/profil-daerah/kondisi-geografis-dan-administrasi-wilayah (2016)

grew about 5.2% per year, causing power crisis and power outages. This power crisis is alleviated with rental generators, which is not an ideal long-term solution. PLN forecasted a growth rate of 8.8% per year, from 217 TWh in 2016 to 457 TWh in 2025 in its RUPTL (Electricity Supply Business Plan) report [4].

PLN (Perusahaan Listrik Negara) is the only state-owned power utility company in Indonesia. In the past, it monopolized the electricity generation, transmission and distribution until the 2009 issuance of Electricity Law, although it still has a right of first refusal over any activity in the sub-sector. Independent Power Producers (IPPs) must sell their generated electricity through PLN, unless they are licensed PPUs (Private Power Utilities) producing for own-use. The majority of power generation is still dominated by PLN. As of 2014, total installed was 53.6 GW with PLN at 37.3 GW (70%), IPP at 11 GW (20%). PPU at 2.5 GW (5%), others with a non-diesel operating license at 2.7 GW (5%) [3].

Indonesia is not a country of meager natural resources either. In the contrary, Indonesia is the fourth-largest coal producer (world's largest coal exporter), tenth-largest gas producer (seventh-largest LNG exporter), and world's largest producer of biofuels. Before 2004, Indonesia was a large exporter of crude oil and member of Organization of the Petroleum Exporting Countries (OPEC) until 2008. Then, it became a net oil importer [1]. The country is blessed with significant power potential from hydro (75,000 MW), biomass (33,000 MW) geothermal (29,000 MW), and solar (4.8 kWh/m_2-day). It holds the largest estimated geothermal reserves in the world or 40% of the total world's reserves [5].

Naturally, as a large coal producer, Indonesia produces its power mostly from coal (44%), the reminder from gas (21%), oil (23%), hydropower (7%) and geothermal power (5%) in 2013 [5]. To expedite the addition of power generation capacity, government issued *Fast-Track Program (FTP I)* in 2006 to rapidly build 10,000 MW coal-fueled power plants, followed by the second 10,000 MW *Fast-Track Program (FTP II)* announced in late 2008 that was predominantly renewable generated power with 40% geothermal. However, in 2013, FTP II target has increased to 17,918 MW with 61% of coal-fired, 28% geothermal, and 10% hydropower plants [1]. Furthermore, in 2015 president Joko Widodo announced plans to accelerate the development of 35 GW program projects. The projects are mostly coal power plants with 5.6 GW of renewable energy projects that includes 1.75 GW geothermal power plants, 2.51 hydro power plants, 1.13 GW bioenergy plants, and remaining 0.233 GW solar and wind energy. Later in August 2015 at a government-run renewable energy convention, the numbers were revised to be 8.75 GW renewable including 2.4 GW geothermal power [3].

1.2. Geothermal Power Generation

Despite having the largest geothermal reserves in the world, Indonesia has only tapped in

5% of its 29,000 MW reserves at 1,400 MW installed capacity. The importance of renewable contribution in the energy mix is more apparent now than ever. The reasons are mounting. Indonesia is the world's sixth largest emitter of carbon dioxide (CO_2) in 2012 or 4.5% global emissions, predominantly coming from power generation sector at 36.4% of all energy related emissions. This sector is experiencing the strongest growth in emissions by 8% per year since 2001 [1]. The country emission is predicted to double from 211 million ton in 2016 to 395 million ton by 2025 with 317 million ton (80%) comes from burning coal. The average emission rate in 2016 was 0.85 $kgCO_2$/kWh, predicted to increase to 0.87 $kgCO_2$/kWh by 2022 due to many coal plants in operation, a delay in hydro and geothermal plants realization and reduced gas use. Later, it is predicted to start decreasing to 0.729 $kgCO_2$/kWh by 2025 due to contributions of gas, geothermal, hydro and other renewables (20% mix), along with using cleaner coal technology. This is in comparison with business-as-usual scenario, in which the emission rate would increase to 0.96 $kgCO_2$/kWh by 2025. With a more aggressive scenario of 25% mix, the emission rate would drop to 0.714 $kgCO_2$/kWh [4].

CO_2 affects directly on climate change and climate change is detrimental globally. Indonesia is most likely vulnerable to climate change. The increase of surface temperature causes rising sea level and flooding in coastal areas of Indonesia. The change in weather patterns brings in more violent monsoon seasons and shifting of dry and rainy seasons affecting fishing industries and farming [6].

Another major concern for the country is energy security and emergency policy. Indonesia has shifted from a large exporter of oil to a net importer after production was dwindling. By 2022, Indonesia could become a net importer of gas due to a number of reasons [5]. Fossil fuel costs can be volatile and unpredictable. Although coal is abundant in Indonesia, it emits the highest CO_2 among other fossil fuels. This is not inline with the national climate change policies and target to reduce carbon emissions.

Following the 2007 Bali Conference, government issued its first general National Action Plan for Climate Change. In 2009 G20 summit in Pittsburg, Indonesia announced a voluntary emissions reduction of 26% (767 million ton (Mt) CO2) by 2020 against business-as-usual scenario and up to 41% (additional 477 $MtCO_2$) with international assistance [1]. Moreover, in 2009, Indonesia issued Environmental Law that includes climate change policies and measures. The law addresses environmental protection and climate change mitigation. Then, the new 2014 National Energy Policy (Kebijakan Energy Nasional) launched an ambitious goal of 23% of renewable to primary energy mix by 2025. The share of renewable has actually fallen from 15% in 2002 to 11.4% in 2012 due to slower growth in hydro and geothermal compared to coal (2.6% and 4.2% respectively). The NEP14 emphasizes the important of energy independence and self-sufficiency. According to roadmap of geothermal

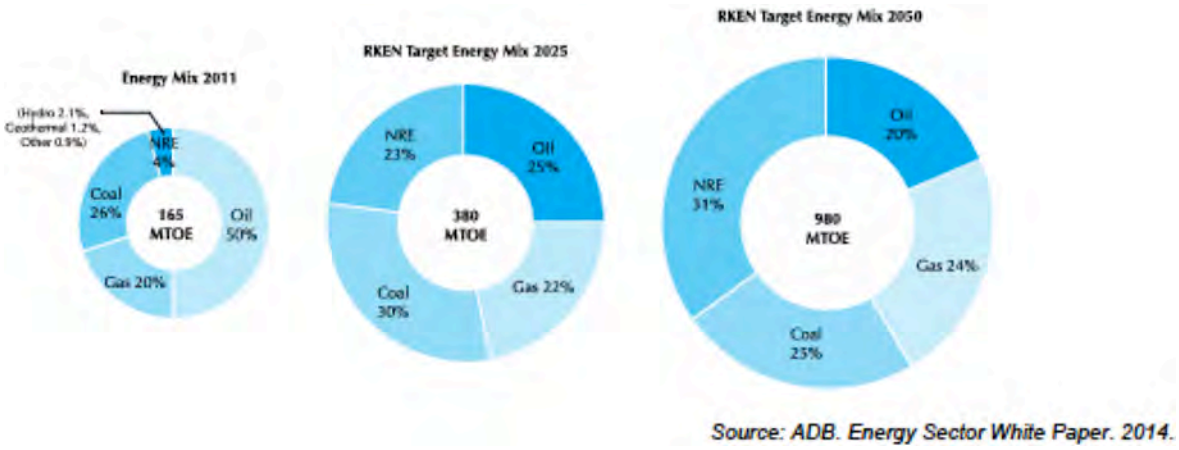

Fig. 1.2 Current and Projected Energy Mix [5]

development, Indonesia aims to install capacity of 6,000 MW by 2020 and 9,500 MW by 2025, although it seems that only 4,000 MW can be expected instead of 6,000 MW by 2020. Under the FTP II, government plans on adding 1 GW of geothermal by 2019 and 4.8 GW by 2024 [1].

Moreover, geothemal power plants are a perfect replacement for coal-fired plants as base load generation with almost 100% of capacity factor. It is “clean” energy emitting 1,800 times less carbon dioxide than coal-fired plants and 1,600 times less than oil-fired power plants [3]. It is economically competitive when avoidance costs on local environment externalities (SO2, NOx, TSP/Total Suspended Particulates), estimated at USD $0.00546/kWh, and global environment externalities (CO2), historically priced between €12-34/ton CO2 from 2005-2010, are considered [7]. Any delay in construction of geothermal power plants would result in more construction of coal-fired plants that will operate for the lifetime duration of 20-25 years.

Additionally, further incentives include the availability of Clean Technology Funding (CTF) established by the global community as available concessional loan for the developers. CTF is part of the USD $6 billion Climate Investment Funds (CIFs) established by the global community to promote activities and investments that would improve climate change [7] [1]. Similarly, International Bank for Reconstruction and Development (IBRD) offers loan rates that may not be as low as CTF but are still better than commercial lending rates [7]. Furthermore, in 2011, Ministry of Finance (MF) established up to $300 million Geothermal Fund that can be used by the government to perform initial drilling and testing of minimum three successful wells prior to tender to relieve initial exploration risks to the developers, hence encouraging more investment participations [8].

Finally, the motive for imperative step toward renewable energy development is the widely accepted global call for 450 scenario to limit the average long-term increase in global

temperature to no more than 2°C compared with pre-industrial levels, which requires limiting the CO2 equivalent concentrations in the atmosphere to no more than 450 parts per million (PPM).

1.2.1. Implementation Challenges

Even though geothermal resources are readily available and government is encouraging the development, the realization of geothermal plants is challenging. In the past, Pertamina Geothermal Energy (PGE), a subsidiary of Pertamina, a state-owned oil and natural gas corporation, was mandated to develop geothermal power generation in Indonesia. However, it was not given the authority to handle the budget by the parent company. Thus, the projects were sitting for a long time without being developed. Later, the projects were bid out to IPPs but there was often lack of interest. The lack of interests was due to many reasons:

1. PLN right to first refusal was a deterrent to many investors [5].
2. The electricity tariff (FIT) was a fixed FIT available to all without consideration of price. Good developers are discouraged by such procedure because they see it as subjective and unreliable [8].
3. No clear and transparent rules that private investment could rely on [1].
4. Developers were expected to assume the exploration drilling, imposing huge initial risks [5].
5. Surface data compiled by Ministry of Energy and Mineral Resources (MEMR) department was often inconsistent and low quality due to limited budget and personnel [5].
6. Land acquisition is lack of clarity and retains poor procedures [1].
7. Geothermal was under forestry law that prohibits mining in the protected forest area where 42% of the geothermal resources are located, unless obtaining president approval adding to the delay [8].
8. Tenders prepared and conducted by local government were often lacking technical clarity, transparency, and unity [8].
9. There was no one-stop shop entity that the developers can go to coordinate and process permits [1].
10. Possible grid connection problems [3].

Government not only faces challenges finding investment but also internal challenges. First, the government subsidizes electricity and fossil fuels. The electricity tariffs are lower than the costs of production. Subsidies have taken much needed resources from state budget to fund critical energy infrastructure, health, and education. In 2013, total energy subsidies accounted for USD $27 billions (11% of state budget expenditures) with $9.0 billions in electric subsidies [1]. Then, there were multiple agencies coordinating the same tasks or policy implementation, yet nobody was put accountable. Often this led to ambitious goals for

only political reasons with no clear plans on how to achieve them. Also, inconsistency in different national plans and policies that were not updated in parallel, making them seem to promote different goals. Moreover, policies and regulations were not applied consistently in the decentralized system. There was no standardization. Lastly, there was a conflict of interest with regulators integrated into the Ministry of Energy or into the state-owned companies. [1]

External challenges included weaker fossil fuel prices that challenged the feasibility of investment in renewable, especially on the smaller scale project where the capital cost per unit of power would be higher [3].

1.2.2. Recommendations to the Challenges

IEA [1] recommended that the government should offer financial incentives for investment, provide transparent price formation, and establish a subsidy reform. It is best if PLN is restructured with separate management and accounting structures with separate reporting and costs between them. This will improve efficiencies. There should be an electric regulator entity that is not part of the ministry or PLN. The ministry and PLN ought to consult with all industry stakeholders, including potential investors, before finalizing the generation capacity plan and transmission forecast to solicit input and avoid unrealistic goals. Government should form and offer a single office that developers can go to and rely on for obtaining information, processing permits, and assist with fast track projects, instead of dealing with different entities and obtain inconsistent information delaying the permitting process. This would in turn streamline the approval process. Government shall improve its day-to-day communication with all the stakeholders. In fact, they also shall improve the communication to the public, campaigning the necessity and timeline of the subsidy reform (phase-out) and the reallocation of the state expenditures to avoid repeating past public resistance and unrest. This should include the compensatory measure plans for the poor. There should not be any delay in policy implementation. Government should develop education programs on geothermal for public, industry, universities, and administrations. It shall analyze and find a way to improve private investment on small-scale geothermal projects up to 10 MW.

Additionally, ADB and The World Bank [8] recommended for 2012 FIT structure to be replaced with tariff ceiling based on PLN's avoided costs. The tariff should be escalated based on starting operation year. The avoided based on three applications:

- Large coal projects of Java-Bali-Sumatra.
- Small coal projects for other islands.
- Diesel projects on remote areas where small coal projects are not feasible.

Government should do the exploration drilling and testing with at least three successful wells

prior to tender. The cost should be recovered from the winning bidder at time of financial closure. Developer should fund and build the transmission connection then handed over to PLN for O&M. Recovery of the cost is through tariff adder over 10 year period. Tender should be executed under a technical qualified central entity representing local government. Significant bid bond and later performance bond should be enforced; thus, would attract only qualified serious bidders. Developers should adopt Australian/Canada geothermal reporting codes for standardization. PLN and Pertamina shall develop separate benchmark for geothermal projects then for oil and gas to avoid competing for budget allocation.

1.2.3. Government Efforts

In light of the recommendations, government applied several improvements. Per ministerial regulation No. 31/2014, electric subsidy is being phased out in stages with a target of 2018, except for the poorest consumers. Geothermal Law was revised in 2014 [3] [8] that include the new ceiling prices (regulation No. 17/2014) and removal of the geothermal classification under mining, enabling geothermal plant development in the protected forest area. The law also revised decentralized system to centralized approval for power generating projects. Government offers incentives for renewable energy generation such as [3]:

- Income tax incentives (a reduction on taxable income, an extended tax loss carry forward, accelerated depreciation and amortization rates, a maximum dividend Withholding Tax of 10%)
- Exemption from Import Duty tax on import of equipment, materials, and capital goods to be utilized in the geothermal projects and/or a facility to produce electricity.
- Import VAT “borne by the government” in the exploration phase of geothermal projects.
- Import VAT exemption for imports of “strategic” capital goods during development/construction phase.

1.3. Sumatra

This study selected Sumatra as the subject of study. The reason being that Sumatra hosts the most abundant geothermal reserves in Indonesia that are located near major demand areas. Sumatra is also one of the 3 major islands under main interconnected grid besides Java and Bali. Therefore, it is an ideal place for geothermal generation projects. It is also to note that the government aims to complete 1,820 MW of new capacity by 2020 in Sumatra, compare to 570 MW in Java/Bali, and 240 MW in eastern islands that are most likely small projects constrained by relatively small loads [8]. Peak demand in 2020 is forecasted to reach 8,500 MW from the 2013 installed capacity of 6,000 MW and expected to increase to about 14,000 MW in 2022. There are also plans for high-voltage direct current (HVDC) links

of Sumatra-Java and Sumatra-Peninsular Malaysia. Alas, many of the large projects are currently delayed causing power shortages and outages [4].

For the last 5 years, Sumatra has experiencing growth of electricity demand higher than average of the country at 9.4% per year. This electricity capacity addition has not met the growing demand with capacity that only grew 5.2% a year. Consequently, it was supplemented by renting generators in 2010. For 2016, PLN arranged more rental generators (2,000 MW) to anticipate power shortages and provide reserve. PLN forecasted

Fig. 1.3 Geographical locations of geothermal resources in Indonesia (source: Geological Agency of Indonesia, MEMR, 2010)

electricity demand in Sumatra would grow from 32.1 TWh in 2016 to 82.9 TWh in 2025 or a growth rate of 11.0% compared to 8.6% average of the country, dominated by residential consumers at 55%. The CO_2 emission of Sumatra is predicted to increase more than double from 29 million ton in 2016 to 66 million ton in 2025. [4]

1.4. Kepahiang Regency

The exact location for this study in Sumatra is in Kepahiang regency. It was selected because of the availability of surface data and its high potential of resource (high temperature).

1.4.1. Geographical location and climate

Kepahiang regency is situated in Bengkulu province, which comprises 8 districts and total area of 66,500 hectare (Ha). Located at position 101°55'19" to 103°01'29" E and 02°43'07" to 03°46'48" S. [9]

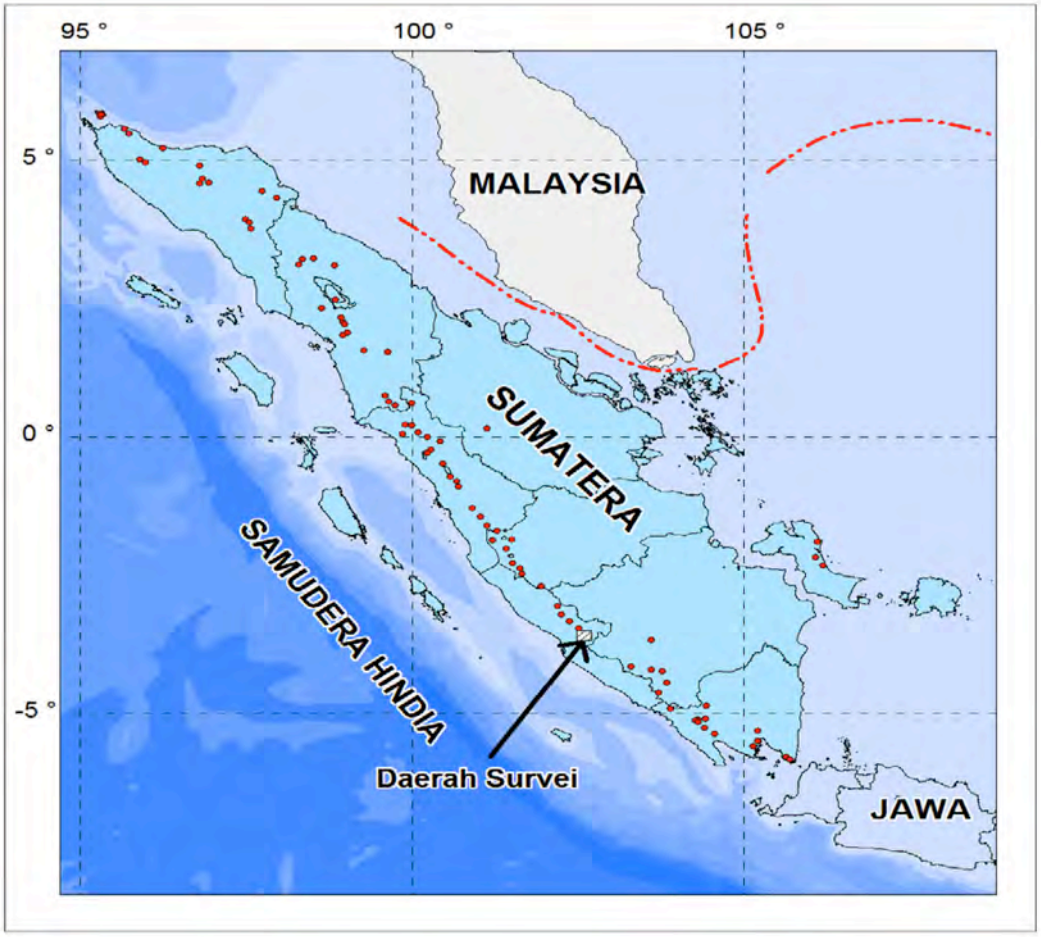

Fig. 1.4 Location of survey Kepahiang, indicated by "Daerah Survey", in Sumatra [25].

It is located at higher elevation with average air temperature around 23.9°C with maximum of 29.9°C and minimum of 19.7°C. The average humidity is around 85% and average rain is approximately 233.5 mm/month[2]. In 2015, the most rain occurred in December at 819 mm and the lowest rain was in July at 25mm [10].

1.4.2. Population and Land Use

In 2015, the population reached at 132,415 habitants at 199/km^2 in average, even though not evenly distributed. The age of 20-64 made 58.7% of the population. Activities were mostly farming. In that year, the recorded paddy field area was 11,195 ha and coffee plantation reached 24,151 ha. [10]

[2] http://kepahiangkab.go.id/index.php/profil-daerah/kondisi-geografis-dan-administrasi-wilayah (2016)

Land use in the area of Kepahiang divided into 4 regions [9]: mountain nature reserve, natural park Kaba mountain, forest, and other land uses. The information regarding status of land use is important for risk anticipation of potential land vulnerability. Anticipation includes applying for permits through proper authority and familiarizing of local society.

1.4.3. Electric Demand

In 2015, the highest electrical connected load came from residential consumers at 28 MVA, followed by industrial and hotels at 3.5 MVA, commercials at 2.4 MVA, offices at 1.9 MVA, and public services at 1.0 MVA [10].

1.4.4. Geological Structure

The geological structure detected in the Kepahiang area is situated in fault line from direction of northwest to southeast, indicated by hills and waterfalls. Geothermal activities that occurred associated with the fault structure trending mainly northeast to southwest and with major active fault zone from Sumatra fault system trending southwest to southeast. [9]

1.4.5. Survey Summaries

The department of geology of the Ministry of Energy and Mineral Resources has completed the following four different surface studies among other previous preliminary studies: Geology and geochemical, geophysics, magnetotelluric, and temperature well. Below are the summaries.

Geology and geochemical [9]l:

- Geothermal system in the Kepahiang area denotes a system of volcanic high relief area.
- Air Sempiang area denotes upflow system and the areas of Babakan Bogor, Suban, Tempel Rejo, and Sindang Jati denote outflow system of the geothermal system Kepahiang (*Fig. 1.5*).
- The source of heat comes from volcanic activities of mount Kaba.
- Cap rock originated from argillic alteration and young lava product around hot spring Sempiang in the area of Bukit Itam with an unknown depth.
- Degree of acidity values or soil pH in the geothermal area Kepahiang ranges between 4.0 – 7.0 and soil temperature at one meter depth is between 20 – 57°C.
- The estimated temperature of the reservoir obtained using gas geothermometer is 250°C, considered as high enthalpy.

Geophysics (gravity, geomagnetic, geoelectric) [11]:

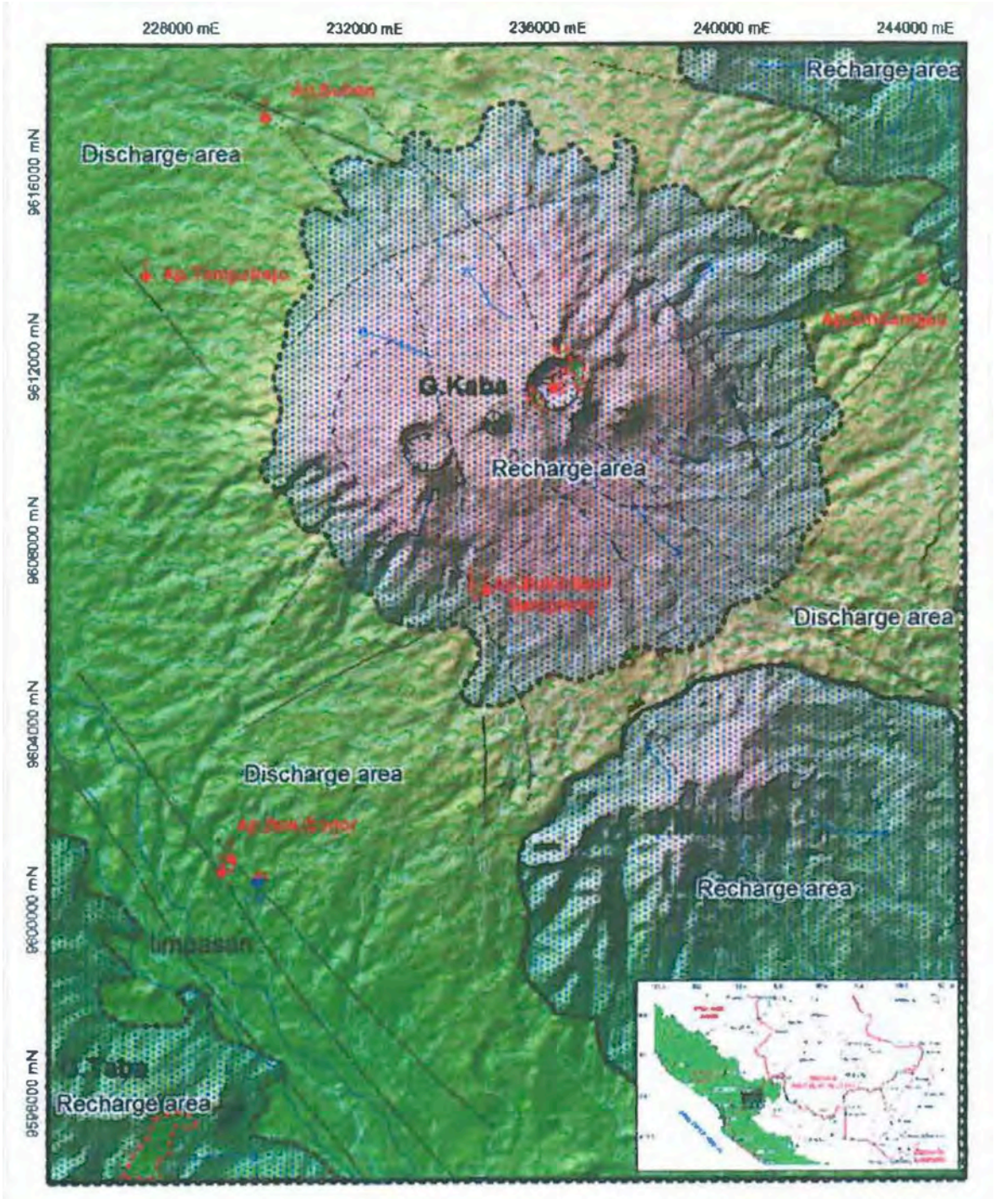

Fig. 1.5 Kepahiang geothermal charge and discharge areas [9].

- Geothermal manifestation area Air Sempiang is dominated by lineaments trending southwest to northwest. It presumed to be the geology fault that created the manifestation.
- The geothermal covering layer has thickness around 300 to 1000 m, layered by volcanic rock product of mount Kaba.

- The reservoir layer has resistivity of 30 Ohm-m and density of 2.5-2.8 gr/cm^3 at the depth of 1500 m below geothermal manifestation Air Sempiang.
- The heat source, based on early Magnetotelluric (MT) data, has resistivity >1000 Ohm-m, with depth >3000 m and likely in a form of residual magma from volcanism of complex Kaba Tua.

Magnetotelluric [12]:

- The cap rock is in a form of alteration rock caused by interaction of hot fluid with rock sources indicated by the low resistivity response.
- The low resistivity response distributed around hot springs Sempiang and extends to the direction of hot spring Babakan Bogor.
- This low resistivity that interpreted as cap rock dispersed from the surface to the depth around 2500 m with thickness approximately 1500 to 2000 m.
- The reservoir estimated to be below the cap rock, which outspreads from hot spring Sempiang to the direction of hot spring Babakan Bogor.
- The top of the reservoir is likely located at the southwest of hot spring Sempiang with depth approximately 1750 m below surface.
- The geothermal prospect area Kepahiahng is estimated around 32 km^2.
- The estimated potential of geothermal after MT measurements is around 180 MWe and categorized as estimated reserve class.

Temperature well [13]:

- The temperature well KPH-1 had a final depth of 452.20 m, located at active volcanic proximate and transition zone of Sumatra fault trench.
- The lithology composed of 1) soil/alluvium, 2) Tuff Breccia at depth 3 - 9 m, 3) Andesite at depth 9 - 26.45 m, 4) Tuff Breccia at depth 26.45 – 65.15 m, 5) Scoria at depth 65.15 – 77.15 m, 6) Tuff Breccia at depth 77.15 – 81.30 m, 7) Andesite at depth 81.30 – 98.40 m, 8) Altered Tuff Breccia at depth 98.40 – 109.35 m, 9) Altered Andesite at depth 109.35 -138.15 m, 10) Altered Scoria at depth 138.15 – 162.60 m, 11) Altered Andesite at depth 162.60 – 169 m, 12) Altered Tuff Breccia at depth 169 – 176 m, 13) Altered Scoria at depth176 – 188.30 m, 14) Altered Basalt at depth 188.30 – 196.20 m, 15) Altered Tuff Breccia at depth 196.20 – 202 m, 16) Altered Basalt at depth 202 – 232.60 m, 17) Altered Tuff Breccia at depth 232.60 – 237.45 m, 18) Altered Basalt at depth 237.45 – 244.90 m, 19) Altered Tuff Breccia at depth 244.90 – 255 m, 20) Altered Andesite at depth 255 – 263.20 m, 21) Altered Tuff Breccia at depth 263.20 – 274 m, 22) Altered Basalt at depth 274 – 356.20 m, 23) Altered Tuff Breccia at depth 356.20 – 381 m, 24) Altered Andesite at depth 381 – 383.20 m, 25) Altered Tuff Breccia at depth 383.20 – 410 m, 26) Altered Basalt at

depth 410 – 452.20 m.

- In general, the altered mineral present dominated with clay minerals type montmorillonite, which could be identified in every rock sample of temperature well KPH-1. Low temperature hydrothermal alteration (montmorillonite) with alteration type argilic, assumed to function as clay cap.
- Petrophysical analysis result, with pores method using mercury, resulted in permeability between 0.20 mdarcy until 143.26 mdarcy, with the highest value from drill sample at depth 410 m. In the meantime, the porosity between 2.39% until 21.53% with the highest value also found in the drill sample of 410 m.
- Heat conductivity measurement from several drilling samples showed 1.43 -1.77 W/mK.
- The initial temperature in the depth of 100 m was 20°C. At depth of 257, the maximum temperature read at 38.20 °C with the Initial Temperature after correction using Horner Plot method was 40.12°C. Then at depth of 380 m, the temperature read at 49.80 °C with the Initial Temperature after correction using Horner Plot method was 52.66 °C. And at depth of 450 m, the temperature read at 75.60°C with the Initial temperature after correction was 107°C.
- Based on the data plotting of the temperature formation at depth 100 m, 257 m, 380 m, and 450 m, it was found the gradient thermal value of 19.11 °C/100 m or about six times the average gradient of the earth (+/- 3°C per 100 m).

1.5. Objectives of the project

With the availability of the surface data but lack of exploration drilling data, this study aims to determine which geothermal power generation technology that may be suitable for Kepahiang geothermal reserve based on the condition of the reserve, power generated, plant efficiency, and economic analysis.

It is hope the study would assist the government in deciding which geothermal technology may be appropriate for the site and expedite the implementation.

1.6. Scope of the project

The study will compare three proposed geothermal power generating technologies: Double-flash cycle, binary cycle, and hybrid single-flash with binary bottoming unit. The comparison will look at the power generated, cycle and plant efficiencies, and finally the economic analysis.

The geothermal technology considered has to be fairly mature technology to minimize risks and maximize expert availability. The hybrid idea is newer compared to the other two but

individually as a single flash and a binary cycle, it is not new.

First, the natural selection for 250°C reserve temperature is to look at double flash or triple flash. Here, the study considers double flash only due to less complication and more mature technology. Single flash is not considered since there will be an excessive exergy wasted by geofluid reinjection at high temperatures to the reservoir (Pambudi et al., 2014, cited by Zeyghami et al. [14]) and alongside, double flash is capable of producing 15-25% more power [15]. One drawback that it is observed in the survey data the geofluid is in the acidic side. The corrosion potential of expensive equipment is higher with the flash plants as the steam goes through every component such as the separator, flasher, turbine, and condenser. Additionally, the vapor phase is high in CO_2 and H_2S. Hence, non-condensable gases treatment system would be required. Also, there is more potential of silica scaling in flash plants [15].

Thus, that brought this study to the second option of binary cycle. In binary cycle, the liquid never changes phase (does not flash), is not released to the atmosphere, does not get in contact with the working fluid, and is injected back to the well almost at the same condition but at lower temperature. Even this reinjection temperature is limited to avoid scaling in the reinjection pipe and evaporator. The only equipment exposed to the corrosion potential is the heat exchangers (pre-heater, evaporator). It is the safest choice in term of scaling, corrosion, and non-condensable gases. The drawbacks include lower power generated and efficiencies. Normally, binary cycle is considered for medium temperature reserve (125-165°C) where flash cycle may not be feasible.

Finally, the last option may offer in-between solution. The third option proposes single flash with binary bottoming unit. This option usually benefits from high temperature reserve similar to a double-flash plant but fewer consequences of scaling, corrosion, and non-condensable gas. Furthermore, DiPippo [15] and also ADB/World Bank joint study [8] have suggested that a bottoming unit could be added at a later time to a single flash unit (or double flash unit). This gives flexibility in term of financial and risks.

1.7. Limitations of the Study

There are significant limitations to the study. Though the site is specific, exploration drilling either has not been performed or if it has, the data has not been made public. Therefore, assumptions were made in the study. The assumptions include general modeling assumptions and also input data assumptions.

The general assumptions for the modeling entail:

- Steady state conditions.

- Changes in potential and kinetic energy and chemical exergies are neglected.
- Heat and pressure losses in all components are neglected.
- Themophysical properties of geofluid are considered as pure water.
- Chemical substances and non-condensable gases are neglected.
- The organic fluid is pure and has the properties of the corresponding material.
- Additional heat from pumps is neglected.

The data assumptions include:

- The dead state temperature T_0 is assumed to be the site web-bulb temperature T_{wb} of 22°C and its corresponding saturated pressure P_0 .
- Geofluid is assumed to remain as liquid in the production well (no flashing) based on the appearances of hot springs. The reservoir pressure is to be calculated based on the reservoir depth.
- Well diameter is chosen arbitrarily based on $13^{3/8}$ inches diameter pipe.

2. Thermodynamic Modeling and Economic Analysis

2.1. Reservoir-Well Modeling

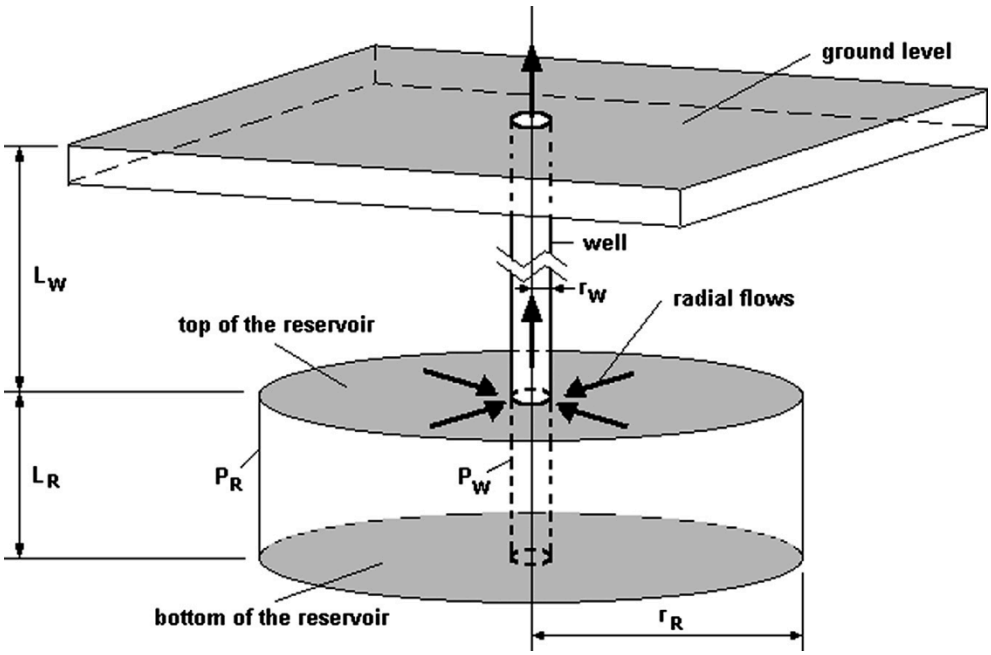

Fig. 2.1 Simplified reservoir-well system schematic. [15]

As mentioned in the list of assumptions in section one, the geofluid arises as pressurized liquid with no flashing occurred inside the well. The reservoir pressure is then calculated as follows:

$$P_R = \rho g(L_w + L_R/2) + friction\ losses \qquad \textit{(Eq. 2.1)}$$

Gravity acceleration *g* is 9.81 m/s^2 and the friction losses are assumed 20%.

Subsequently, the head pressure of the well P_H [15] is calculated at incremental mass flow rates.

$$P_H = P_R - C_d\dot{m} - C_2 L_w \dot{m}^2 - \rho g L_w \quad \textit{(Eq. 2.2)}$$

$$C_d = \frac{\mu \ln\left(\frac{r_p}{r_y}\right)}{2\pi K H \rho} \quad \textit{(Eq. 2.3)}$$

$$C_2 = \frac{8f}{\rho \pi^2 D^5} \quad \textit{(Eq. 2.4)}$$

2.2. Double Flash Plant Modeling

By the end of 2014, double-flash steam plant made up 9.4% of all geothermal plants or 54 plants in 10 countries [15]. In this study, dual admission turbine system is assumed, depicted in *Fig. 2.2*. From a production well PW, the geofluid passes through silencer S and wellhead valve WV where the pressure is lowered to a flashing point. Then, it goes a cyclone separator CS where the geofluid is separated into steam and liquid. The high pressure steam then proceed toward the turbine T/G through a moisture remover MR and several valves, while the liquid goes to a flash vessel F after reducing its pressure further by a throttle valve TV to once again flash into steam and some liquid. The lower pressure steam enters the dual admission turbine. The expanded steam leaves the turbine to a condenser C to be cooled with cool water CW from a cooling tower. Finally, the condensed geofluid is injected back into the well with a condensate pump CP.

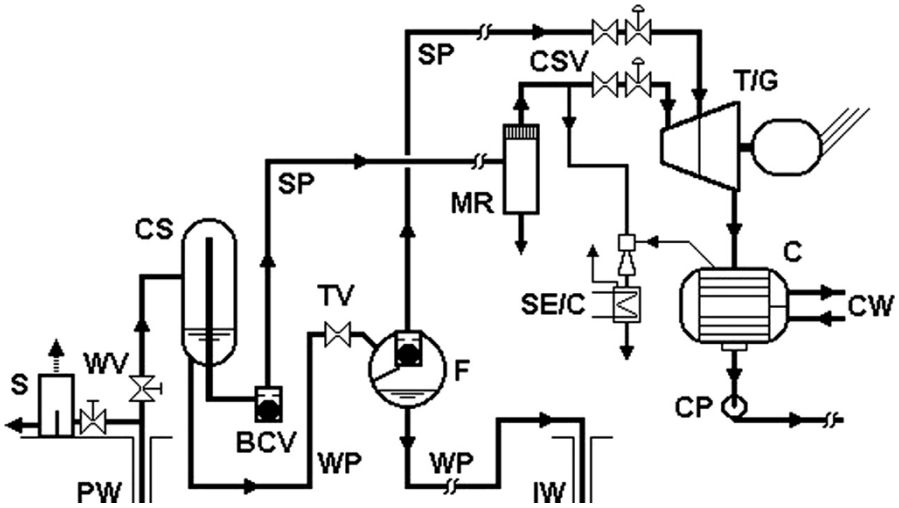

Fig. 2.2 Simplified double-flash power plant schematic. [15]

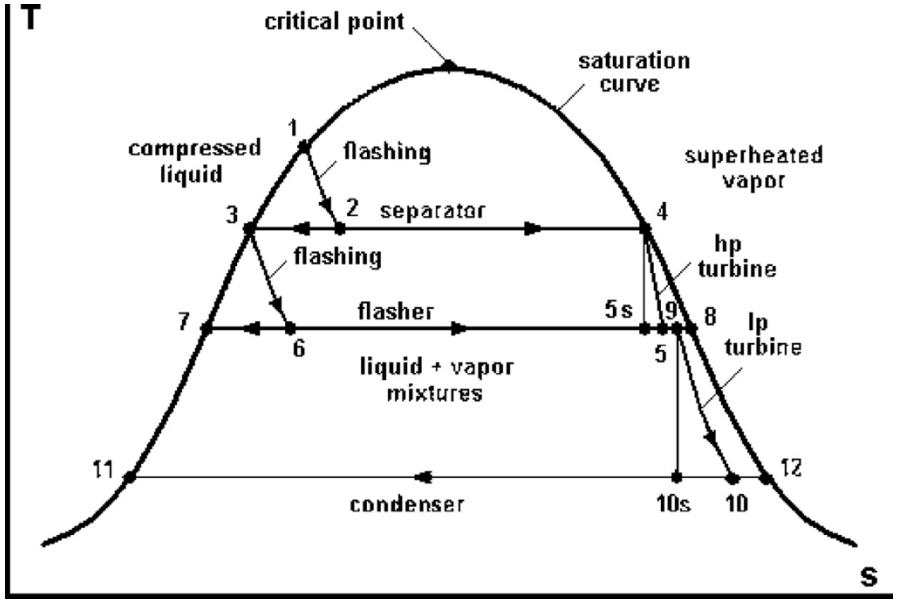

Fig. 2.3 Temperature-entropy process diagram for double-flash plant with a dual-admission turbine. [15]

The method of the modeling is by applying a control volume at each process and applying the first law of thermodynamic of mass and energy balances. The temperature-entropy diagram is shown in *Fig. 2.3*. The following equations are taken from the *Geothermal Power Plant* book authored by Ronald DiPippo [15].

2.2.1. At Geofluid Separator Vessel

Through a control valve, the pressure of incoming resource geofluid is lowered to a flashing point, where it flashes spontaneously under adiabatic condition and goes to a separation process at point 2.

$$h_1 = h_2 \qquad \textit{(Eq. 2.5)}$$

At the separation pressure, P_2, the steam quality can be found as:

$$x_2 = \frac{h_2 - h_3}{h_4 - h_3} \qquad \textit{(Eq. 2.6)}$$

where h_3 is the saturated liquid enthalpy and h_4 is saturated vapor enthalpy at P_2 and its corresponding saturated temperature T_2.

2.2.2. At Geofluid Flash Vessel

From the separator, the liquid goes to a flash vessel where the pressure is reduced further adiabatically and some liquid vaporized into steam subsequently.

$$h_3 = h_6 \qquad \textit{(Eq. 2.7)}$$

And the low-pressure steam quality at P_6 and its corresponding saturated temperature T_6 is as follows:

$$x_6 = \frac{h_3 - h_7}{h_8 - h_7} \qquad \textit{(Eq. 2.8)}$$

2.2.3. Conservation of Mass

Based on conservation of mass, mass balances can be calculated as follows:

$$\dot{m}_{hps} = x_2 \dot{m}_{total} = \dot{m}_4 = \dot{m}_5 \qquad \textit{(Eq. 2.9)}$$

$$\dot{m}_{hpb} = (1 - x_2)\dot{m}_{total} = \dot{m}_3 = \dot{m}_6 \qquad \textit{(Eq. 2.10)}$$

$$\dot{m}_{lps} = (1 - x_2)x_6 \dot{m}_{total} = \dot{m}_8 \qquad \textit{(Eq. 2.11)}$$

$$\dot{m}_{lpb} = (1 - x_6)(1 - x_2)\dot{m}_{total} = \dot{m}_7 \qquad \textit{(Eq. 2.12)}$$

2.2.4. Turbine Analysis

During the expansion in the turbine, the steam quality drops below 100% and starts to develop a little amount of moisture. The moisture causes degradation in the performance of the turbine and hence the decline of isentropic efficiency. The so-called Baumann rule calculates the actual exit enthalpy from the turbine, h_5. [15]

$$h_5 = \frac{h_4 - A\left[1 - \frac{h_7}{h_8 - h_7}\right]}{1 + \frac{A}{h_8 - h_7}} \qquad \textit{(Eq. 2.13)}$$

$$A = 0.425(h_4 - h_{5s}) \qquad \textit{(Eq. 2.14)}$$

$$h_{5s} = h_7 + (h_8 - h_7)\left[\frac{s_4 - s_7}{s_8 - s_7}\right] \qquad \textit{(Eq. 2.15)}$$

where h_{5s} is the ideal exit enthalpy if the process is isentropic or reversible.

The high-pressure steam enters the turbine. The power generated and turbine efficiency can be found as:

$$w_{hpt} = h_4 - h_5 \quad \textit{(Eq. 2.16)}$$

$$\dot{W}_{hpt} = \dot{m}_{hps} w_{hpt} \quad \textit{(Eq. 2.17)}$$

$$\eta_{hpt} = \frac{h_4 - h_5}{h_4 - h_{5s}} \quad \textit{(Eq. 2.18)}$$

The outlet steam at state 5 then mixes with the low-pressure steam from the flasher at state 8, ready to enter the low-pressure turbine at state 9. Enthalpy at state 9 can be found as:

$$h_9 = \frac{x_2 h_5 + (1 - x_2) x_6 h_8}{x_2 + (1 - x_2) x_6} \quad \textit{(Eq. 2.19)}$$

and the conservation of mass will be

$$\dot{m}_9 = \dot{m}_5 + \dot{m}_8 \quad \textit{(Eq. 2.20)}$$

$$\dot{m}_5 h_5 + \dot{m}_8 h_8 = \dot{m}_9 h_9 \quad \textit{(Eq. 2.21)}$$

The turbine outlet condition, state 10, can be analyzed using the Baumann rule. Due to the quality of the steam at state 9 is wet or less than 1, then the value of x_9 has to be used [15].

$$h_{10} = \frac{h_9 - A\left[x_9 - \frac{h_{11}}{h_{12} - h_{11}}\right]}{1 + \frac{A}{h_{12} - h_{11}}} \qquad \text{(for } x_9 < 1\text{)} \quad \textit{(Eq. 2.22)}$$

$$A = 0.425(h_9 - h_{10s}) \quad \textit{(Eq. 2.23)}$$

$$h_{5s} = h_7 + (h_8 - h_7)\left[\frac{s_4 - s_7}{s_8 - s_7}\right] \quad \textit{(Eq. 2.24)}$$

Then, the low-pressure turbine power generated and efficiency can be estimated as follows:

$$w_{lpt} = h_9 - h_{10} \quad \textit{(Eq. 2.25)}$$

$$\dot{W}_{lpt} = \dot{m}_9 w_{lpt} \quad \textit{(Eq. 2.26)}$$

$$\eta_{hpt} = \frac{h_4 - h_5}{h_4 - h_{5s}} \quad \textit{(Eq. 2.27)}$$

Finally, the total power generated and gross electrical power are computed as follows:

$$\dot{W}_{total} = \dot{W}_{hpt} + \dot{W}_{lpt} \quad \textit{(Eq. 2.28)}$$

There are two constraints that the expanded steam quality at state 5, x_5, and at state 10, x_{10}, should be ≥ 0.85. Otherwise, the large droplets could damage the mechanical blades. [16]

2.2.5. Condenser Analysis

The expanded steam leaves the turbine and enters the condenser to be cooled back to liquid to be injected back into the injection well. The mass flow rate required of cold water would depend on the temperature rise, ΔT. Since there is no phase change of the cooling water and a small range of temperature difference, a constant specific heat of water of 4.2 kJ/kg K $\bar{c}_p$ can be used instead of enthalpy.

$$\dot{m}_{cw} = (\dot{m}_5 + \dot{m}_8)\left[\frac{h_{10}-h_{11}}{\bar{c}_p \Delta T}\right] \qquad \textit{(Eq. 2.29)}$$

For a direct contact condenser $\Delta T = T_{11} - T_{cw}$.

Yet, this study compares between different geothermal plant technologies and DiPippo pointed out that the cooling tower relative size between binary and flash power are relatively the same at equal capacity, which is about 8.5 times larger than a conventional plant [15]. Therefore, cooling tower analysis will not serve as a comparison in this study and will not be implemented here.

2.2.6. Utilization Efficiency

Utilization Efficiency is a good parameter for a comparison in environmental and economic study. Second Law of Thermodynamic is applied by comparing the actual net plant power with the maximum theoretical power could be produced with the given geofluid through exergy calculation. The specific exergy is determined as such:

$$e = h(T,P) - h(T_0,P_{0)} - T_0[s(T,P) - s(T_0,P_0)] \qquad \textit{(Eq. 2.30)}$$

where T_0 is the dead-state temperature of the geofluid (e.g., the local wet-bulb temperature if using a water cooling tower), while h_0 and s_0 are values at T_0.

The maximum theoretical power is specific exergy multiplied by geofluid mass flow rate:

$$\dot{E} = \dot{m}_{total} e \qquad \textit{(Eq. 2.31)}$$

Hence, below defines the utilization efficiency or the exergetic efficiency:

$$\eta_u = \frac{\dot{W}_{net}}{\dot{E}} \qquad \textit{(Eq. 2.32)}$$

2.3. Binary Plant Modeling

By the end of 2014, Binary plants comprised 35% of all plants in operation or 203 plants in 15 countries. The units are generally small at 6 MW/unit although larger units of 15-22 MW

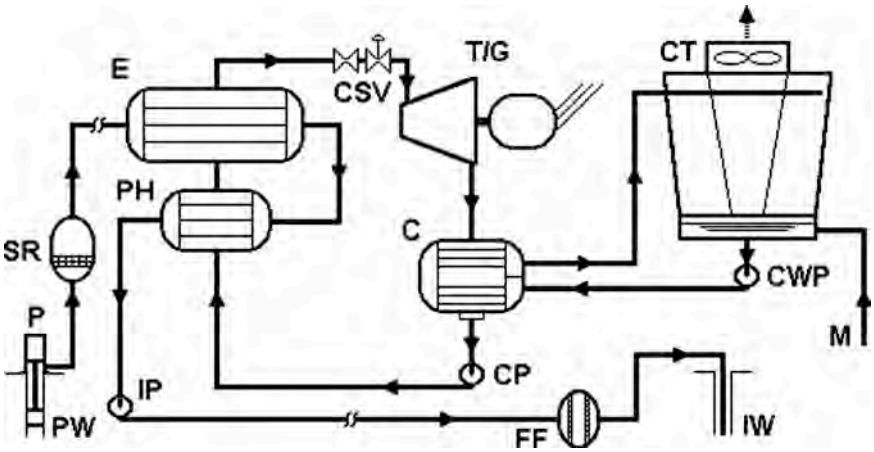

Fig. 2.4 Simplified binary power plant schematic. [15]

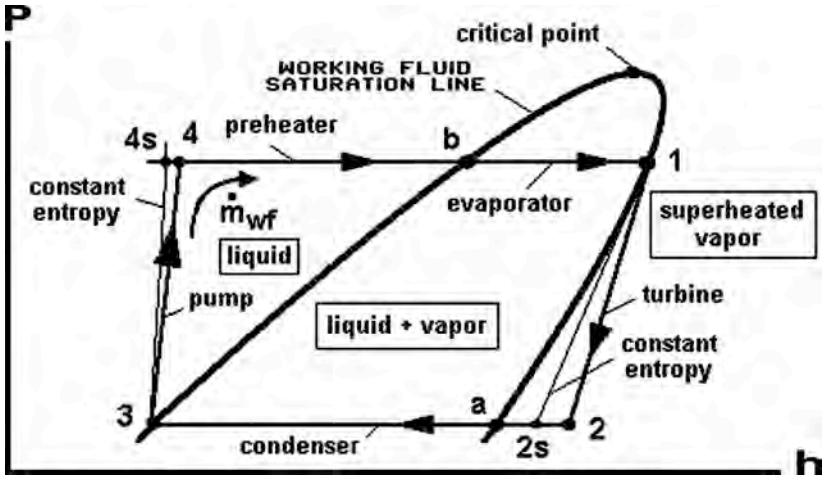

Fig. 2.5 Pressure-enthalpy diagram for a basic binary plant. [15]

with advanced cycle design are coming soon. Thus despite being most widely used, they only generated 10.4% of the total power or 1245 MW. [15]

Fig. 2.4 illustrates simplified layout of a binary plant. A well pump P located in the production well PW below the flash depth that is determined based on the fluid properties and flow rate desired drives the geofluid through a sand remover SR, if needed to remove any impurities that may damage the piping and heat exchanger tubes, and enters an evaporator E. In the evaporator, the heat transfers from the hot geofluid to the working fluid to bring it to the change phase stage from boiling point to vapor. Leaving the evaporator, the geofluid now enters a preheater PH, transferring the heat remaining to the working fluid to bring it to its boiling point. From there, the geofluid is now ready to return back to the injection well (IW) with an injection pump IP and through a final filter FF.

In parallel, the working fluid goes through a rankine cycle of preheating at the preheater, boiling to vapor state at the evaporator, expanding at the turbine generating power (T/G), and

finally cooling down back to the liquid state at the condenser C, which rejects its heat to an air cooling tower or water cooling tower. Now, the cooled down working fluid is ready to be pumped (CP) to increase its pressure and repeats the cycle.

The pressure-enthalpy diagram is illustrated in *Fig. 2.5*. One may find the following thermodynamic balances in DiPippo's *Geothermal Power Plant book* [15]. Again, a control volume is applied for each component to analyze the energy and mass balances.

2.3.1. Turbine Analysis

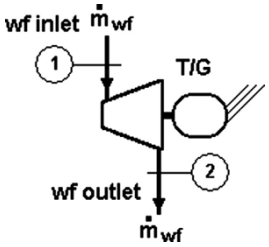

By applying a control volume around the turbine component, the generated power can be analyzed as such:

$$\dot{W}_t = \dot{m}_{wf}(h_1 - h_2) = \dot{m}_{wf}\eta_t(h_1 - h_{2s}) \qquad \textit{(Eq. 2.33)}$$

Turbine efficiency η_t value is known.

2.3.2. Condenser Analysis

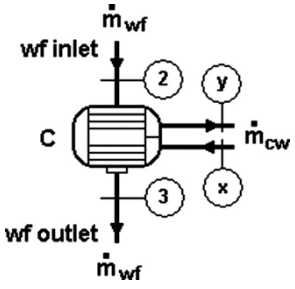

Heat rejected to the cooling water (or air) is as follows:

$$\dot{Q}_c = \dot{m}_{wf}(h_2 - h_3) \qquad \textit{(Eq. 2.34)}$$

The energy balance between the working fluid and cooling medium is therefore:

$$\dot{Q}_c = \dot{m}_{cw}(h_y - h_x) = \dot{m}_{cw}\bar{c}_p(T_y - T_x) \qquad \textit{(Eq. 2.35)}$$

Again, the cooling water specific heat $\bar{c}_p$ can be assumed constant for a small range of temperature difference and no phase change.

2.3.3. Condensate Pump Analysis

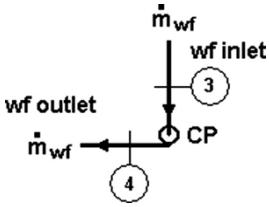

The pump work can be found as such:

$$\dot{W}_p = \dot{m}_{wf}(h_4 - h_3) = \dot{m}_{wf}(h_{4s} - h_3)/\eta_p \qquad \textit{(Eq. 2.36)}$$

Pump efficiency η_p is known.

2.3.4. Preheater and Evaporator Analysis

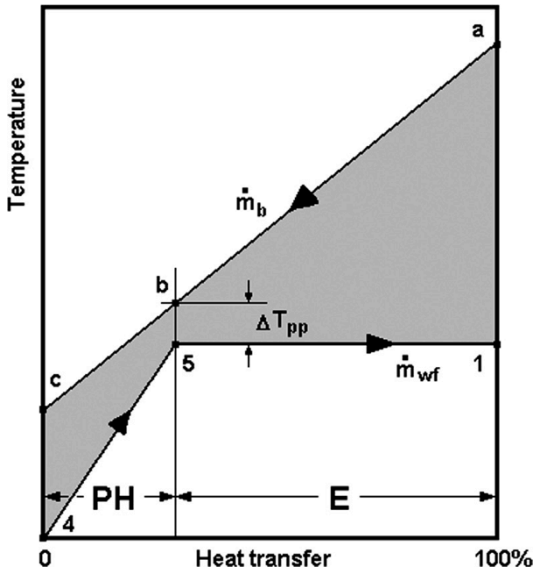

Fig. 2.6 Pinch point temperature. [15]

The preheater increases the temperature of the working fluid to a boiling point. Then, the evaporator gives the heat input for the working fluid to evaporate into vapor. The point in the heat exchanger where the working fluid experiences the closest temperature to the geofluid is called pinch point temperature difference or ΔT_{pp}, which normally happened at the hot end of the preheater/cold end of the evaporator.

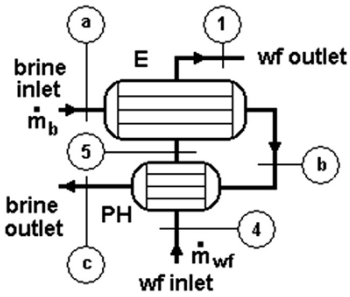

The energy balance in the heat exchangers can be establish as:

Preheater: $\dot{m}_b \bar{c}_{p,b}(T_b - T_c) = \dot{m}_{wf}(h_5 - h_4)$ *(Eq. 2.37)*

Evaporator: $\dot{m}_b \bar{c}_{p,b}(T_a - T_b) = \dot{m}_{wf}(h_1 - h_5)$ *(Eq. 2.38)*

2.3.5. Overall Cycle Analysis

Net power generated would be:

$$\dot{W}_{net} = \dot{W}_t - \dot{W}_p$$

The thermal efficiency as a gauge of the cycle performance can be calculated as such:

$$\eta_{th} = \frac{\dot{W}_{net}}{\dot{Q}_{PH+E}} \qquad \textit{(Eq. 2.39)}$$

The heat rejection ratio over net power generated is

$$\frac{\dot{Q}_c}{\dot{W}_{net}} = \frac{1}{\eta_{th}} - 1 \qquad \textit{(Eq. 2.40)}$$

2.3.6. Utilization Efficiency

The second law of thermodynamic analysis to measure utilization efficiency or exergy efficiency of the plant is accomplished the same way as the double flash plant:

$$\eta_u = \frac{\dot{W}_{net}}{\dot{E}} = \frac{\dot{W}_{net}}{\dot{m}_b[(h_{res} - h_0) - T_0(s_{res} - s_0)]} \qquad \textit{(Eq. 2.41)}$$

2.4. Single-Flash with Binary Bottoming Unit Modeling

There are a few different arrangements of flash-binary hybrid plants. In this study, the arrangement such as *Fig. 2.7* will be assumed, in which the geofluid liquid after the steam separator is utilized in a binary cycle before it returns to the injection well.

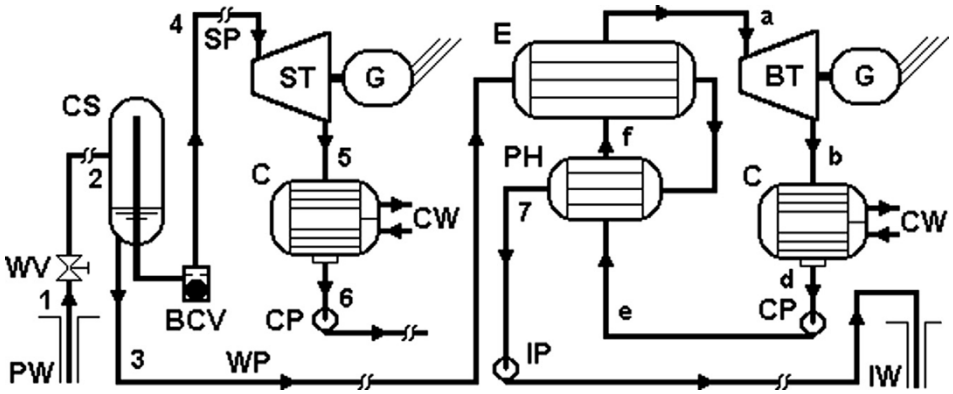

Fig. 2.7 Single-flash with binary bottoming unit [15]

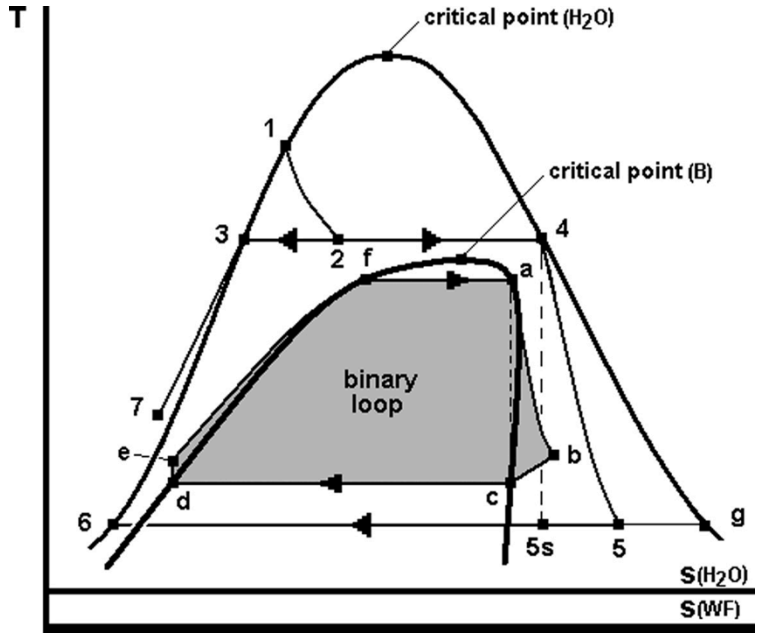

Fig. 2.8 Temperature-entropy diagram for single-flash with binary bottoming unit [15]

The thermodynamic analysis is no other than a combination of single flash and binary cycle plant. In the previous section double flash and binary cycle have been covered and the analysis processes can be used similarly.

The binary cycle working fluid may be calculated using the First Law energy balance:

$$\dot{m}_{wf}(h_a - h_e) = \dot{m}_b(1 - x_2)c_{p,b}(T_3 - T_7) \qquad \textit{(Eq. 2.42)}$$

$$\dot{m}_{wf} = \dot{m}_b(1 - x_2)c_{p,b}\frac{(T_3 - T_7)}{(h_a - h_e)} \qquad \textit{(Eq. 2.43)}$$

2.5. Economic Analysis

A simple economic analysis is performed to give an idea of the order of economic benefits in lieu of actual predicting the real costs or actual pay back year. Net present value (NPV) method is used:

$$NPV = \sum_{t=1}^{T}\frac{C_t}{(1+r)^t} - C_o \qquad \textit{(Eq. 2.44)}$$

C_t = net cash flow during the period of t
C_o = total initial investment costs
r = discount rate
t = number of time periods

3. Results and Discussions

Below table contains the reservoir data and themophysical properties that were used for the modeling.

Table 3.1 Reservoir data and thermophysical properties.

Reserve Pressure (Pa)	P_R	18811656
Absolute Viscosity (Pa*s)	μ	0.000106
Permeability (m^2)	K	3E-14
Reservoir thickness (m)	L_R	1000
Well diameter (m)	r_w	0.1695
Reservoir area (km^2)	A_R	32
Reservoir radius (m)	r_y	3192
Density (kg/m3)	ρ	799
Well coefficient of friction ()	f	0.01
Well diameter (m)	D	0.339
Geofluid Temperature (°C)	T_b	250
Geofluid saturated pressure (bar)	P_s	39.73
Well depth (m)	L_W	1500

3.1. Modeling Results

3.1.1. Double-Flash Plant Results

First, the head pressure P_H of the well was calculated at incremental brine flow rates. The minimum pressure before flashing at the given reserve temperature T_R was reached at 39.95 bar (Table 3.2).

Next, a control valve of flow factor K_v of 9000 m3/h/√bar reduced the pressure to flashing point before entering the separation vessel. Note that the lowest P_2 possible was 4.34 bar as the lower limit should not be lower than 1 bar to prevent air from being sucked inside the separator. The highest possible pressure within flashing range was 36.50 bar. Therefore, this was the range to work with (Table 3.2).

Table 3.2 Double-flash calculated working range of pressure and temperature.

m_b [kg/s]	P_H [Bar]	P_2 [Bar]	T_2 [°C]	h1 = h2 [kJ/kg]
30	66.36	66.18	280.0	1248
40	64.95	61.77	275.6	1241
50	63.53	58.57	270.0	1233
60	62.11	54.96	265.0	1226
70	60.68	50.95	265.0	1218
80	59.24	46.54	255.0	1210
90	57.80	41.72	250.0	1201
100	56.35	36.50	242.6	1193
110	54.89	30.88	235.0	1184
120	53.43	24.85	222.9	1175
130	51.96	18.42	208.3	1166
140	50.48	11.58	185.7	1157
150	49.00	4.34	145.5	1148
160	47.50			
170	46.01			
180	44.50			
190	42.99			
200	41.47			
210	39.95			

The conditions below were assumed for the calculations:

Table 3.3 Double-flash design parameters.

Condenser pressure (bar)	P_c	0.1
Condenser temperature (°C)	T_c	45.8
Electrical generator efficiency	η_g	96%

The flash temperatures T_6 (Table 3.4) were selected using the "equal-temperature-split" [15] between the separator temperature and the condenser temperature. The pressures P_6 are the corresponding saturated pressures. The expanded steam qualities leaving the turbine, x_5 and x_{10}, all satisfied the requirement of ≥ 0.85.

Table 3.4 Double-flash power generated and utilization efficiency.

m_b [kg/s]	P_2 [Bar]	T_2 [°C]	T_6 [°C]	P_6 [Bar]	x_5	x_9	$W_{e,gross}$ [MW]	w_e [kJ/kg]	η_u	Q_o/W_e
100	36.50	242.6	144.2	4.01	0.88	0.97	13.32	133	0.48	4.05
110	30.88	235.0	140.4	3.61	0.89	0.96	14.73	134	0.49	4.05
120	24.85	222.9	134.4	3.01	0.89	0.96	16.22	135	0.49	4.09
130	18.42	208.3	127.1	2.41	0.90	0.95	17.72	136	0.49	4.16
140	11.58	185.7	115.7	1.61	0.91	0.95	19.13	137	0.50	4.38
150	4.34	145.5	95.6	0.85	0.93	0.95	18.95	126	0.46	5.20

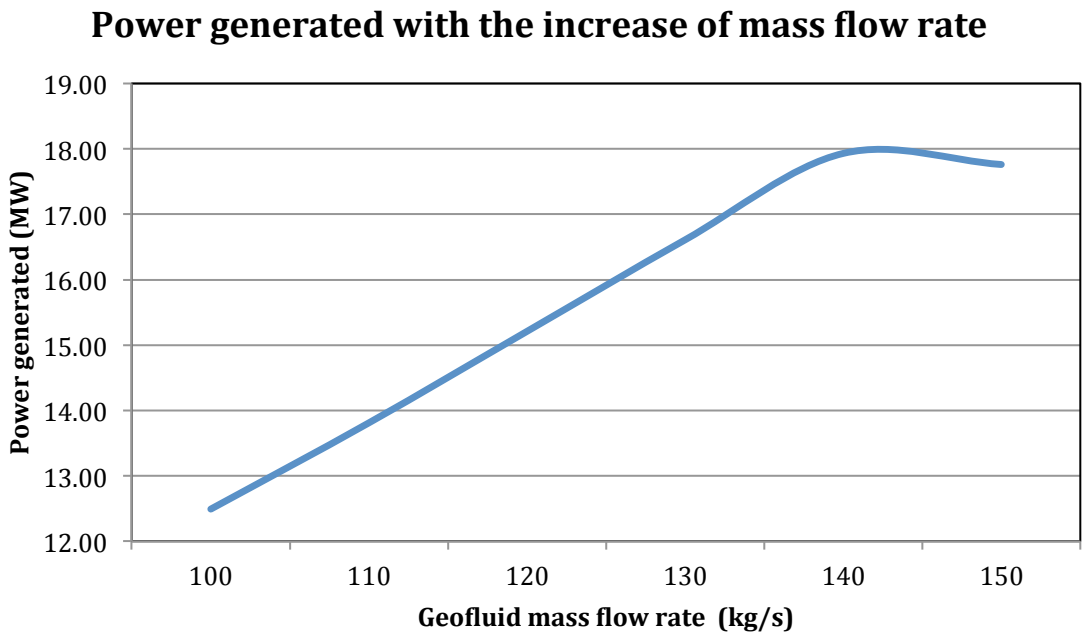

Fig. 3.1 Power generated with the incremental increase of geofluid mass flow rate

The results (Table 3.4) show that the power generated, specific power, and utilization efficiency all happened to peak at the same mass flow rate, although this is not always the case. Sometimes the highest power generated does not give the highest utilization efficiency nor specific power, which then one has to choose which is more important for the project [15]. Last column shows the heat rejection ratio. As pointed out by DiPippo [15], geothermal plant cooling tower could be 8.5 times the size of the conventional plant cooling tower.

3.1.2. Binary-Cycle Plant Results

The modeling of the binary plant started similarly as the double-flash plant. The head pressures at the incremental flow rates had been calculated. Unlike double-flash plant, the thermal efficiency or utilization efficiency does not change with the increase in flow rate (subsequently well-head pressure) in binary plant, granted that all other conditions stay the same including the working fluid. Therefore, to compare the three technologies, brine mass flow rate of 140 kg/s (P_H of 46.72 bar) was used to calculate the power and efficiencies.

The conditions below were assumed for the calculations:

Table 3.5 Binary-cycle design parameters.

Isentropic turbine efficiency	η_t	85%
Isentropic pump efficiency	η_p	75%
Condenser HX efficiency	η_c	90%
Electrical generator efficiency	η_g	96%

First, the reinjection temperature was introduced. After a few trial-errors of different temperatures, it settled at 70°C. It cannot be any lower than this to avoid scaling problems [14] [17]. The heat exchangers were assumed counter flow arrangement, shell and tube.

Hydrocarbons, classified as dry fluid, were the preferred working fluids owing to their positive slope. Hence, the working fluid expands in the turbine under the superheated region and no moisture would degrade the turbine. Refrigerants, classified as isentropic fluid with infinite slope, were disregarded in this study for their harsher impacts on the environment and therefore, their restrictions by the Montreal protocol. Yet, hydrocarbon fluids are not without faults, such as being flammable. However, this is not a problem if proper precautions are taken. [15] [14] [17]

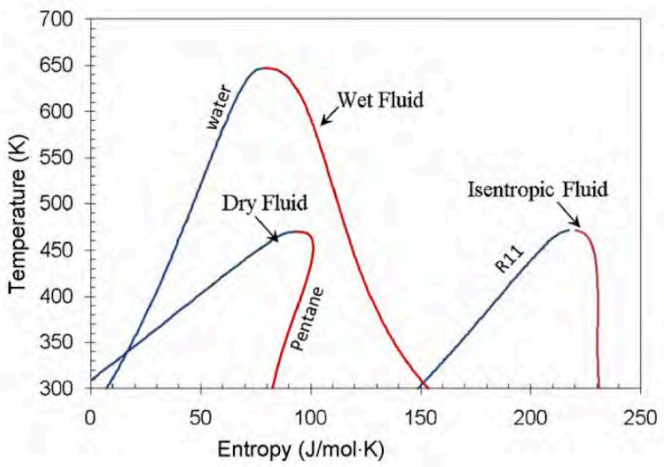

Fig. 3.2 T-S diagram of dry, isentropic, and wet fluid. [18]

The hydrocarbon fluids considered in this study were pentane, isopentane, and butane. The study included trial-error modeling of the different fluids and varying the evaporator and condenser conditions within limits. The limits required the separator pressure to be no lower than 100 kPa and condenser pressure to be no lower than 13.5 kPa (DiPippo, 2008 cited by Zeyghami et al in [14]). The condenser temperatures selected were at 30 and 40°C. Meanwhile, the evaporator pressures were at 20 and 25 bar (not to exceed maximum allowable temperature of 127°C for butane and 177°C for pentane and isopentane [15]). The trials included different combination of these temperatures and pressures.

The working fluids performance was gauge by the (smaller) pinch-point temperature T_{pp} ,

(larger) power generated, and (larger) exergy/utilization efficiency. As it turned out, it was significantly difficult to achieve T_{pp} within 5°C. It was in fact impossible while maintaining the heat exchange efficiency to no more than 98%. Additionally, some trials might show smaller T_{pp} but also lower exergy efficiency or power. Ultimately, it was decided that the exergy and power take precedent over T_{pp} . Poor matching of the geofluid curve with the working fluids could cause this Tpp difficulty. One example, the geofluid temperature is considered high temperature at 250°C. Normally, medium temperature geofluid applications (< 200°C) utilize binary-cycle plants. When working fluid maximum temperature allowable is 127 and 177°C, the slope of the geofluid heat transfer in the heat exchanger would have to be fairly steep (lower geofluid exit temperature).

The best match from the trials pointed to Pentane at 20 bar evaporator pressure and 30°C condenser temperature as found by Liu et al. [19]. The higher critical temperature of pentane compare to isopentane and butane might contribute to this. Yet, the T_{pp} remained no where close to 5°C at 22°C while Zeyghami et al. [14] pointed out that the highest source of exergy loss is in the evaporator and suggested that the one place to improve the system efficiency is the evaporator. Furthermore, using a mixture working fluid would improve the temperature profile match between the two fluids.

Table 3.6 Pentane thermodynamic properties at selected conditions

State	P [Bar]	T [K]	h [kJ/kg]	s [kJ/kg K]
State 3	0.82597	**303.15**	126.352	0.45783
State 4s	**20**	303.642	129.468	0.45783
State 5	**20**	436.387	489.306	1.4302
State 1	**20**	436.387	690.262	1.8907
State2s	0.82597	346.986	566.055	1.8907
State a			486.534	
State 4	20.00	304.08	130.507	
State 2	0.82597		584.686	

The state numbering on Table 3.6 is referring to *Fig. 2.5*. The bold numbers are known conditions. State 4s and 2s are ideal conditions (isentropic).

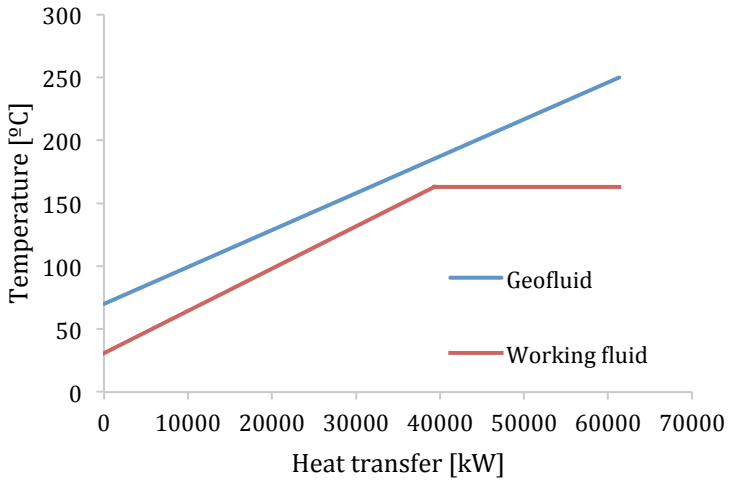

Fig. 3.3 Temperature-heat transfer diagram for preheater and evaporator

The results of the modeling are summarized in Table 3.7. Thermal efficiency is higher than suggested by DiPippo [15] at 10-13% and this is before other parasitic loads are subtracted. The power per mass flow rate is lower than the double-flash plant as expected with less power generated. The utilization efficiency is a lot less than the double-flash plant indicating more exergy destruction. The heat rejection ratio is similar between the two plants as mentioned by DiPippo [15].

Table 3.7 Binary-cycle modeling results

Preheating heat transfer [MW]	Q_{PH}	39.33
Evaporator heat transfer [MW]	Q_E	22.03
Geofluid heat input [MW]	Q_{Geo}	61.36
Turbine power generated [MW]	Q_t	11.57
Condenser heat rejection [MW]	Q_c	50.24
Pump work [MW]	W_p	0.46
Net (thermal) Power [MW]	W_{net}	11.12
Electrical Power [MW]	$W_{e,gross}$	**10.66**
Specific Power [kW/kg/s]	w_e	**76.11**
Heat rejection ratio	Q_c/W_{net}	**4.52**
Thermal efficiency [%]	η_{th}	**18.12%**
Utilization/exergy efficiency [%]	η_u	**27.61%**

3.1.3. Single-Flash with Binary Bottoming Unit Results

Like the other previous two, the modeling applied the same general conditions. Furthermore as decided in the binary unit above, the focus was more on the geofluid mass flow rate of 140 kg/s for the purpose of comparison. Nonetheless, the study ran the entire range of feasible flow rates to see if 140 kg/s still presented the optimal results.

Using the same well-head pressures as in section 3.1 (Table 3.2), the modeling started with the single-flash plant. The design parameters likewise followed the double-flash modeling conditions (Table 3.3). The results are summarized in Table 3.8.

Table 3.8 Single-flash modeling results.

$m_{b,1}= m_{b,2}$ [kg/s]	P_2 [Bar]	T_2 [°C]	x_5	$W_{e,flash}$ [MW]	η_u
100	36.50	242.6	~~0.81~~	-	-
110	30.88	235.0	~~0.82~~	-	-
120	24.85	222.9	~~0.82~~	-	-
130	18.42	208.3	~~0.83~~	-	-
140	11.58	185.7	0.85	13.88	0.36
150	4.34	145.5	0.88	16.19	0.39

First of all, it could be noted that the same selections of separator pressure P_2 as the double-flash modeling may not be the optimal pressure selections for the single-flash modeling. This is for the reason that the condenser pressure and temperature stayed the same in both cases. In the case of the double flash, there was an intermediate pressure of the low-pressure turbine. Hence, the steam outlet condition at state 5 from the high-pressure turbine was maintained within the constrained of $x_5 \geq 0.85$. Meanwhile, in the single-flash modeling, there was no intermediate pressure. Consequently, the expanded steam started to fall below 0.85 as indicated in Table 3.8. As suggested by DiPippo [15] and repeated by Zeyghami et al. [14], the optimum separator temperature (corresponding to the saturated pressure) is approximately the average of the geofluid incoming temperature and condenser temperature:

$$T_{separator} = 0.5(T_{geofluid} + T_{condenser})$$

Applying the above estimation with the geofluid temperature at 250°C and condenser at 46°C, then the separator temperature would have to be around 148°C. This is inline with the results where the optimum power generated and utilization efficiency occurred at T_2 *of* 145.5°C. Nevertheless, the study proceeded with comparing the 3 plant technologies at the mass flow rate of 140 kg/s. Yet, one could keep in mind that each technology could be optimized further with the right selection of pressure and temperature among other parameters explicitly for that technology.

Ensuing, the study only looked at the performance of those within the constraint conditions, which left only two flow rates at 140 and 150 kg/s. When comparing to the single-flash optimal power at 16.2 MW, the double-flash optimal at 19.1 MW produced 18% more power than the single-flash cycle. DiPippo suggested 15-25% [15] more power and Karsdottir et al. [16] cited Dagdas (2007) of 20-25% more power.

Proceeding to the bottoming unit, the conditions used by the binary cycle were applied (Table 3.5). The working fluid selections were again the hydrocarbons pentane, isopentane, and butane. Similarly, the separator pressures modeled were at 20 and 25 bar and condenser temperatures were 30 and 40°C. Trial errors of different combinations of pressure and temperature with each hydrocarbon narrowed down the selection to butane this time as the best option. Although when aforementioned the best, it was not optimal given that once again it was difficult to achieve a pinch-point temperature any closer to 5°C. Nonetheless, it was closer than at the binary-cycle case at T_{pp} around 12-13 °C (Table 3.10). A closer temperature profile match between the two fluids most likely contributed this. The geofluid this time entered at 186°C and 146°C in lieu of a high 250°C as in the binary-cycle case. The reinjection temperature was limited to no lower than 70°C to avoid silica scaling in the piping and evaporator. However, 70°C is not always the case. In some cases it could be a higher safe limit. It would all depend on the geofluid silica concentrations [15]. Therefore, it is critical to study the geofluid chemical compositions beforehand.

Below are the thermodynamic properties of butane at the best combinations. The lettering corresponds to *Fig. 2.8*. The bold numbers are known conditions. State es and bs are ideal conditions (isentropic).

Table 3.9 Butane thermodynamic properties at selected conditions

State	P	T	h	s
State d	2.81357	**303.15**	165.633	0.61932
State es	**20**	303.515	168.647	0.61932
State f	**20**	387.875	395.313	1.27437
State a	**20**	387.875	629.158	1.87726
State bs	2.81357	318.556	547.684	1.87726
State c			518.966	
State e	20.00	303.929	169.652	0.62263
State b	2.81357	325.007	559.905	1.91524

Table 3.10 Binary bottoming unit results.

m_b [kg/s]	m_3 [kg/s]	$P_2 = P_3$ [Bar]	$T_2 = T_3$ [°C]	T_{pp} [°C]	$W_{e,binary}$ [MW]
140	114.13	11.58	185.7	12.1	8.25
150	112.30	4.34	145.5	12.7	2.46

Mass flow rate $\dot{m}_3$ is the liquid portion of geofluid from the separator, where the vapor went to the flash cycle. Unlike the single-flash part of the hybrid, the binary-cycle part produced more power for the incoming fluid of 140 kg/s. Below are the two corresponding temperature-heat transfer diagrams for the preheater and evaporator.

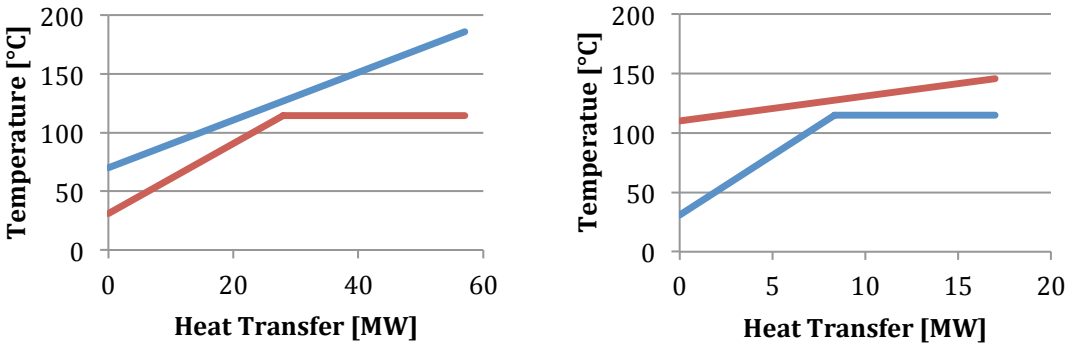

Fig. 3.4 Temperature-heat transfer diagram for preheater and evaporator at 140 kg/s and 150 kg/s well mass flow rate.

Table 3.11 Single flash with binary bottoming unit results.

$m_{b,1} = m_{b,2}$ [kg/s]	$W_{e,Total}$ [MW]	w_e [kW/kg/s]	η_u	Q_o/W_e
140	21.63	154	0.56	4.69
150	18.50	123	0.45	5.07

The total of the combination single flash-bottoming binary unit is summed up in Table 3.11. Although the single flash cycle showed the peak power at mass flow rate of 150 kg/s, yet it was not enough to supersede the low power generated by its bottoming binary unit pair. At the end, the mass flow rate 140 kg/s produced more total power and higher utilization efficiency. In fact, this third option performed the best out of the three technologies in comparison, in power generated, utilization efficiency, and naturally, the specific power. On a final note, the heat rejection ratio is again about the same magnitude as the previous two. This confirmed that cooling tower modeling was not crucial for the purpose of this study.

3.1.4. Plant Modeling Summary

Below figures summarize the modeling. Hybrid single-flash with binary bottoming unit succeeds over the other two. Karlsdottir et al. [16] also discovered in their study that the exergetic efficiency for the hybrid single flash and binary is utmost compare to the other cycles. This could be favorable for Kepahiang application.

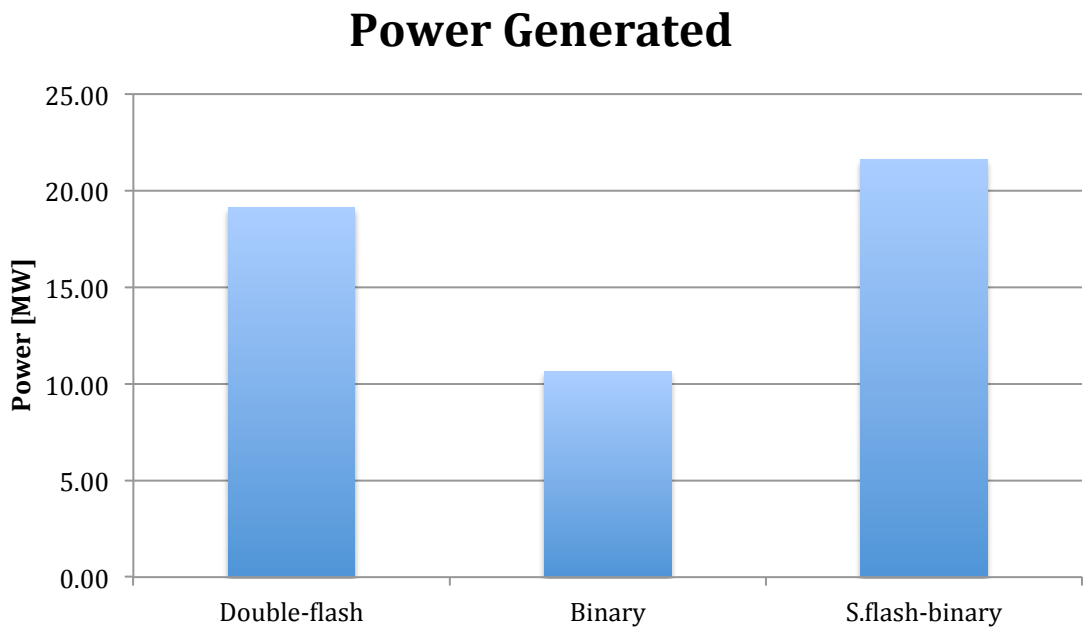

Fig. 3.5 Power generated comparison.

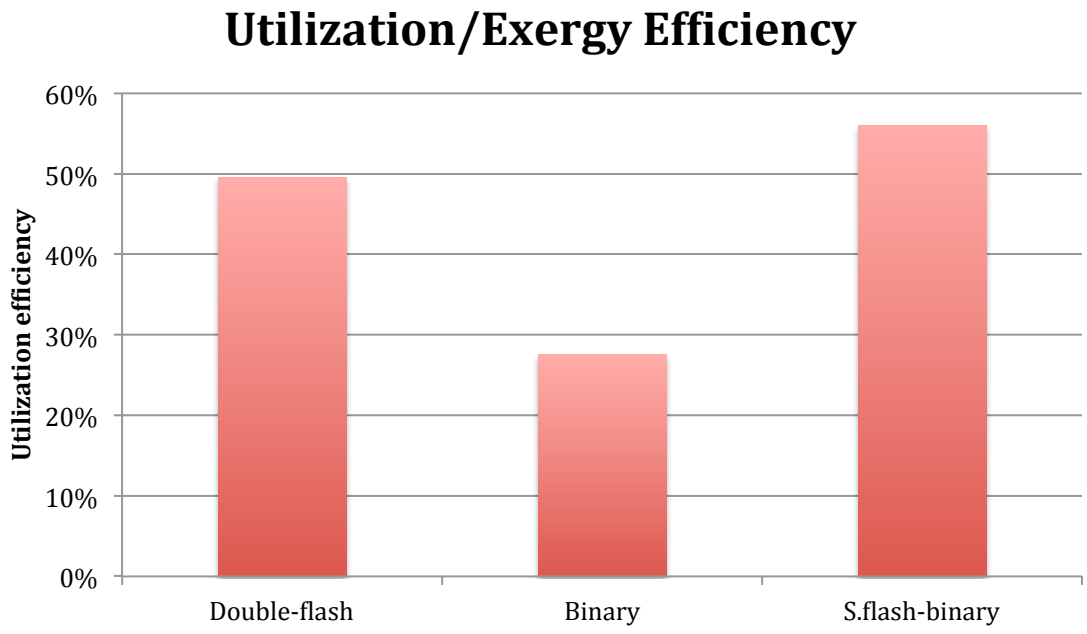

Fig. 3.6 Utilization efficiency comparison.

3.2. Economic Analysis Results

It is to note that the economic results are for comparison purposes only instead of to price out the cost of each technology. The reason is because the actual cost would require further economic and site study. Geothermal costs are site specific. It depends on the resource

temperature, number of wells, site access, and chemical compositions. As the resource temperature increases, the same equipment would produce more energy and therefore, the cost per kW would decrease [20]. Well costs account for more than half of the capital costs [20]. Sites that are hard to access such as remote locations with the lack of infrastructure will drive up the installation costs. Furthermore, some chemical compositions may require non-condensable gas extraction, corrosive protecting liner, or scale treatment.

Up to the present time, there is still inconsistency on the costs of geothermal plants. A few sources cited binary plant costs as higher than flash plant costs [21] [22], which may be based solely on the plant efficiency and energy produced as mentioned above. Yet, California Energy Commission (CEC) [20] found that the actual costs from of flash plants might be higher. It replaced its *2009 Integrated Energy Policy Report (IEPR)* with *2013 Integrated Energy Policy Report (IEPR)*, where the double-flash costs were noticeably increased in comparison. In *2009 IEPR*, binary costs were higher than flash plant and it was vice versa in the 2013 IEPR. As quoted [20], "the expected costs of these projects seem to have underestimated the actual costs encountered as this technology undergoes its first major domestic investment surge in more than 15 years."

Energy Information Administration (EIA) came out with the 2013 *Updated Capital Cost Estimates for Utility Scale Electricity Generating Plants* listing double-flash costs as higher than binary costs as well, although it is considerably higher including its listing of O&M in comparison with the cost differences stated by CEC [23]. EIA listed flash plant overnight capital cost at $6,243/kW and binary at $4,362/kW (2012$) and CEC instant mid cost case listed at $6,041 and $5,342 (2013$) for flash and binary respectively. EIA suggested $132/kW-year for flash plant O&M costs and $100/kW-year (2012$) for binary plant, while CEC estimated the same O&M costs for both flash and binary at $89.79/kW-year (2013$). EIA modeled the cost estimates based on site-specific sources. [20] [23]

These costs were in 2012 and 2013 dollars. The study assumed a start operation of 2021, four years from today. Based on the recommendation by Stefansson [24] for a stepwise development strategy, developing a geothermal field would be typically takes 6 years from the preliminary survey. The steps recommended include preliminary survey/reconnaissance (1 year), surface exploration (1 year), exploration drilling (1 year), and production drilling and power plant (3 years). Preliminary survey and surface exploration for Kepahiang reserve have been completed. Thus, the next step would be exploration drilling. Asian Development Bank (ADB) and World Bank suggested for the government to do the drilling and testing prior to tender with at least 3 successful wells to minimize risks to the developers and consequently, attract investors [8]. This cost is to be recovered from the successful bidder at a time of financial closer of the project [8].

Although the most accurate way to normalize the costs from 2012 or 2013 dollar to 2021 is to

apply a price index such as Producer Price Index (PPI), such price index specific to geothermal was not readily available. One way to do is to breakdown the costs and to apply the price index for each component. For example US Bureau of Labor Statistics has price index for well drilling, equipment, material, and services. The challenge entailed not knowing the details such as number of wells, equipment sizes, if non-condensable gas remover, scaling treatment, or corrosive protection liner is required, etc. This would require further investigation and design.

Nevertheless, as mentioned above the purpose of the study is to compare the three technologies and not to price out. Therefore, the study applied across the board 3% escalation for the capital costs and 0.5% escalation for the O&M per year. The discount rate applied was only an estimate. In actuality, developers desire a higher discount rate, which is entirely possible with a combination of tariff negotiation, securing highly concessional loans from Climate Technology Fund (CTF) and International Bank for Reconstruction and Development (IBRD), and applying for carbon credit [7].

This study used the costs from CEC. The CEC costs were based on different peer studies. Thus, it listed low cost case, mid cost case, and high cost case as collected from these previous studies. CEC also summarized both instant costs and installed costs. Instant costs include all costs plus land and permitting costs. Installed costs are instant costs plus the cost of financing the plant during construction, sales tax, and development fees [20]. This study took the installed costs by merchant at mid cost case and O& M costs also at mid cost case as the average costs (Table 3.12, Table 3.13).

The electricity cost used for the calculation was obtained from the third edition (2015) of *Power in Indonesia: Investment and Taxation Guide*, a report prepared by Price Water House Coopers (PwC) Indonesia [3]. The electricity costs are in a form of ceiling prices that was recommended by The World Bank and ADB in a joint study [8], in lieu of the previous feed-in tariff. Ceiling prices encourage competition and lowest possible prices while still remain attractive to developers. The ceiling prices were formulated based on avoided costs of large coal projects in large interconnected grids of Sumatra, Java Bali, small coal projects in smaller grids of other islands, or diesel generators on islands where small coal projects are not feasible. Sumatra is under region 1 (Table 3.14). The prices are based on the plant's commercial operation date.

Table 3.12 CEC Summary of 2013 Instant and Installed Costs [20]

Capital Costs Year = 2013 (Nominal Dollars)	Instant Costs ($/kW)	Installed Costs ($/kW)		
		Merchant	IOU	POU
Mid Cost Case				
Binary Geothermal 30 MW	$5,342	$7,099	$7,228	$6,486
Flash Geothermal 30 MW	$6,041	$7,747	$7,863	$7,196
High Cost Case				
Binary Geothermal 30 MW	$8,869	$10,055	$10,260	$9,493
Flash Geothermal 30 MW	$8,189	$11,560	$11,764	$11,000
Low Cost Case				
Binary Geothermal 30 MW	$4,410	$5,098	$5,176	$4,926
Flash Geothermal 30 MW	$3,816	$4,350	$4,408	$4,222

Table 3.13 CEC Summary of Operating and Maintenance Costs [20]

O&M Costs Year = 2013 (Nominal Dollars)	Fixed O&M ($/kW-Yr)	Variable O&M ($/MWh)
Mid Cost Case		
Geothermal Binary 30 MW	$89.79	$0.00
Geothermal Flash 30 MW	$89.79	$0.00
High Cost Case		
Geothermal Binary 30 MW	$154.78	$0.00
Geothermal Flash 30 MW	$182.58	$0.00
Low Cost Case		
Geothermal Binary 30 MW	$89.79	$0.00
Geothermal Flash 30 MW	$86.15	$0.00

Table 3.14 Geothermal tariffs - Ceiling Prices [3]

COD	Ceiling Price (USD cents/kWh) for geothermal power projects		
	Region 1	Region 2	Region 3
2015	11.8	17.0	25.4
2016	12.2	17.6	25.8
2017	12.6	18.2	26.2
2018	13.0	18.8	26.6
2019	13.4	19.4	27.0
2020	13.8	20.0	27.4
2021	14.2	20.6	27.8
2022	14.6	21.3	28.3
2023	15.0	21.9	28.7
2024	15.5	22.6	29.2
2025	15.9	23.3	29.6

3.2.1. Double-Flash Economic Analysis Results

With the generated power as summed up in Table 3.4, the calculated energy production, costs, and revenues are summarized in Table 3.17.

The capacity factor was based on the CEC report [20] for mid case value. The high capacity factor makes geothermal plant suitable for a base plant. The feed-in tariff was using the ceiling price of starting operation year of 2021, even though it is acknowledged that in competitive bidding, this price may be lower. For the purpose of the calculation, the study used the ceiling price. These parameters are summarized in Table 3.16.

Flash cycle plant generates a little bit of carbon dioxide CO_2 emissions though trivial in comparison with fossil-fuel plants. The average emission value reported in CEC report was 264.5 lbh/MWh or 120.0 kg/MWh. At this time, carbon emission charges have not been applied in Indonesia. If $20/ton emission charge was to be applied, then the payback time set back another 2 years.

Table 3.15 Double-flash plant with CO_2 emission cost.

CO_2 emissions [kg/MWh]	120.0
CO_2 emissions/year [Tons]	16,973
CO_2 cost/ton	$20
CO_2 cost/year	$339,467
Total revenue with CO_2/year	$17,974,384

Table 3.18 displays the net present values showing payback time of 25 and 27 years. The focus, nevertheless, is not on the number of years since a few things could be altered. For example, the installed costs may be different depending on geographic location and site conditions. Government incentives and tax breaks have not been applied. The escalation rates of the costs may not be as high as assumed. The focus, however, will be in the order of magnitude.

3.2.2. Binary-Cycle Economic Analysis Results

With generated power as shown in Table 3.7, the energy, costs, and revenues were calculated as presented in Table 3.17.

Again, the study used the mid case value capacity factor in CEC [20] report. Also, the feed-in tariff was the ceiling price for the 2021 starting operation year with awareness that in actuality the price may be lower resulted from competitive bidding (Table 3.16)

Binary plants do not generally emit CO_2 except in one study, CEC [20] found small emission, which was categorized in high case. This study followed the mid case of no CO_2 emissions

Its net present values are shown in Table 3.18. Payback period is 20 years, which therefore economically stands more attractive than the double-flash plant.

3.2.3. Flash-Binary Hybrid Economic Analysis Results

Capacity factor and feed-in tariff stayed the same (Table 3.16). Carbon dioxide was not evaluated due to insufficient information. With the generated power summarized in Table 3.11, the production, costs, and revenues are presented in Table 3.17.

CEC has not covered the cost for single flash with binary bottoming unit and neither, EIA. Coskun et al. [21] priced combined cycle flash/binary in between double flash cycle and binary cycle for medium temperature geothermal sources. Due to absence of costs, the analysis applied the costs from both double flash and binary to compare. With the double-flash costs, the hybrid analysis is marked as “hi” and marked as “lo” with the binary costs.

Using the double flash cost, the NPV values are almost the same as the double flash with a 25-year payback but with a slight more gain than the double flash. In the meantime using the binary costs, the results are also about the same as the binary with a 20-year payback with again a slight more gain than the binary. The net present values are shown in Table 3.18.

3.2.4. Economic Analysis Summary

Table 3.16 Economic Parameters for all plants

Start operation year	2021
Capacity Factor CF	85%
Feed in Tariff (2021) [$/kWh]	0.142
Escalation rate (capital)/year	3%
Escalation rate (O&M)/year	0.5%
Discount rate	8.5%

Table 3.17 Energy produced, costs, and revenues.

	Flash	Flash + CO2	Binary	Flash/Binary Hi	Flash/Binary Lo
Installed size [MW]	19	19	11	22	22
Production/year [MWh]	141,474	141,474	81,906	163,812	163,812
Income/year [$M]	$20,089	$20,089	$11,631	$23,261	$23,261
Installation cost/kW (2013$)	$7,747	$7,747	$7,099	$7,747	$7,099
O&M cost/kW/year (2013$)	$89.79	$89.79	$89.79	$89.79	$89.79
Installation cost [$M]	$186,460	$186,460	$98,921	$215,901	$197,842
O&M cost/year [$M]	$1,775	$1,775	$1,028	$2,056	$2,056
CO2 cost/year [$M]	-	$339.47	-	-	-
Total revenue/year [$M]	$18,314	$17,974	$10,603	$21,206	$21,206

In *Fig. 3.7*, it shows that binary plant case has the lowest investment and could achieve the highest NPV during the lifetime of the plant. If the hybrid flash/binary plant was to have the same costs as the binary plant ("flash/binary lo"), then the net present values surpass the binary plant by year 19 with more revenues generated (steeper slope). If the hybrid plant was to have the double-flash plant costs, then it has the highest investment but surpasses the double flash plant by year 25 in term of net present values although it is still slightly below the binary plant curve. It may be safe to assume that if the costs of hybrid were in between the double-flash and the binary costs, then its net present values would be greater than both plants. Karlsdottir et al. [16] found in their study that hybrid flash-binary is more economically viable than the double flash cycles for enthalpies under 1300 kJ/kg. At higher enthalpies, the double flash becomes more economically viable. This study also has enthalpies below 1300 kJ/kg.

Table 3.18 Net Present Values (NPV) comparison between plants.

Year	1	2	3	4	5	6	7	8	9	10	11	12	13
Flash	-169.58	-154.02	-139.69	-126.47	-114.29	-103.07	-92.72	-83.18	-74.40	-66.30	-58.83	-51.95	-45.61
Flash+CO_2	-169.89	-154.63	-140.55	-127.58	-115.63	-104.61	-94.46	-85.10	-76.47	-68.52	-61.20	-54.44	-48.22
Binary	-89.15	-80.14	-71.84	-64.19	-57.14	-50.64	-44.65	-39.13	-34.04	-29.35	-25.03	-21.05	-17.38
Flash/Binary Hi	-196.36	-178.34	-161.74	-146.44	-132.34	-119.34	-107.36	-96.32	-86.14	-76.76	-68.12	-60.15	-52.81
Flash/Binary Lo	-178.30	-160.28	-143.68	-128.38	-114.28	-101.28	-89.30	-78.26	-68.08	-58.70	-50.06	-42.09	-34.75

14	15	16	17	18	19	20	21	22	23	24	25	26	27	28	29	30
-39.76	-34.38	-29.41	-24.84	-20.62	-16.73	-13.15	-9.85	-6.80	-4.00	-1.41	0.97	3.16	5.19	7.05	8.77	10.36
-42.48	-37.20	-32.32	-27.83	-23.69	-19.88	-16.36	-13.12	-10.13	-7.38	-4.84	-2.51	-0.35	1.64	3.47	5.15	6.71
-13.99	-10.87	-8.00	-5.35	-2.91	-0.66	1.42	3.33	5.09	6.71	8.21	9.59	10.86	12.03	13.11	14.11	15.03
-46.04	-39.81	-34.06	-28.76	-23.87	-19.37	-15.23	-11.40	-7.88	-4.63	-1.64	1.12	3.66	6.01	8.17	10.16	11.99
-27.98	-21.75	-16.00	-10.70	-5.82	-1.31	2.83	6.66	10.18	13.43	16.42	19.18	21.72	24.07	26.23	28.22	30.05

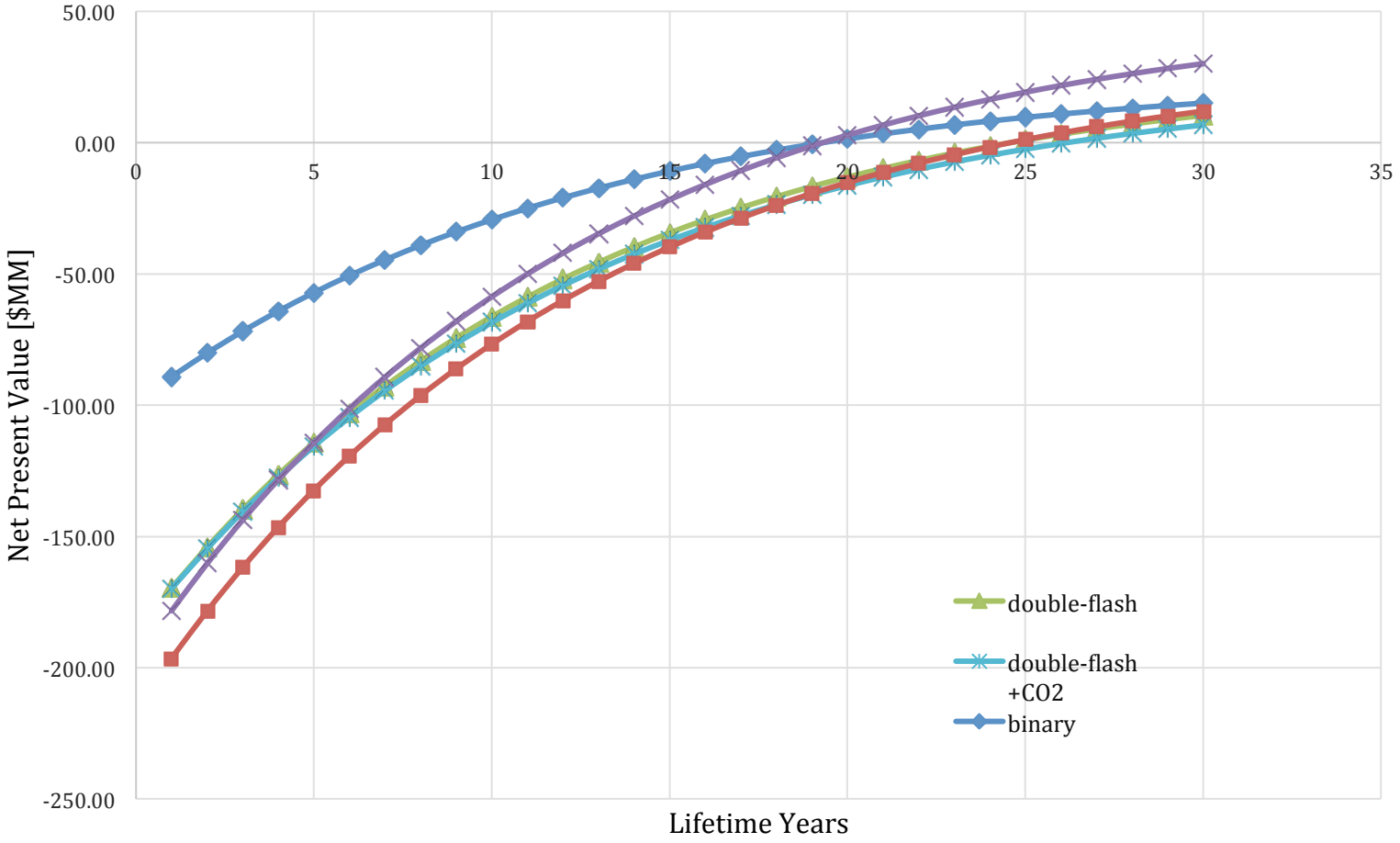

Fig. 3.7 Net Present Value (NPV) curves of all plants.

Conclusions

In conclusion, hybrid single-flash with binary bottoming unit may be an excellent choice for Kepahiang reserve. In this case, it shows highest power generated among the three and this is considering that the working fluid was not optimal. When the working fluid is re-selected with an optimal mixture, then the results may be even greater. In term of the utilization efficiency, the hybrid plant also wins over the other two options making it an obvious selection. This does not always happen. Often times, highest generated power does not coincide with highest utilization efficiency. Then, one has to choose which parameter is more important.

The cost analysis, however, is inconclusive, although it is safe to assume that the cost will be between the binary plant and the double flash plant as also found in the study by Karlsdottir et al. for enthalpies under 1300 kJ/kg. If this is the case, it is possible that the net present value of the hybrid in its lifetime is greater than the other two. Even though binary plant shows possibly the highest NPV in this calculation, binary plant offers low generated power and efficiencies. With the financing concern of small projects below 10 MW in Indonesia, it may not be a good selection, unless there is an absolute concern over pipe and equipment scaling and corrosion with the flashing cycle. This could be determined further after exploration drilling and testing.

Another advantage of bottoming binary plant is that the unit is modular. When, in the future, the temperature and pressure of the reserve is dropping, the binary unit could be removed if necessary. On reverse, as mentioned before, the bottoming binary unit could be added at a later time to an existing flash plant. This may minimize initial risks on financing.

Finally, there are more ways to further improve the results such as adding recuperator for double-flash plant or hybrid plant, between the geothermal brine and steam at the high-pressure turbine outlet [16] [19], and different hybrid arrangements [15].

Bibliography

[1] INTERNATIONAL ENERGY AGENCY (IEA), "Indonesia 2015: Energy Policies Beyond IEA Countries,".

[2] ASIAN DEVELOPMENT BANK, "Achieving Universal Electricity Access in Indonesia," e-ISBN 978-92-9257-269-3, 2016.

[3] PRICEWATER HOUSE COOPERS (PwC) INDONESIA, "Power in Indonesia: Investment and Taxation Guide, 3rd Edition ," 2015.

[4] PT PERUSAHAAN LISTRK NEGARA (PLN), "Rencana Usaha Penyediaan Tenaga Listrik (RUPTL): Tahun 2016 - 2025," 2016.

[5] ASIAN DEVELOPMENT BANK, "Summary of Indonesia's Energy Sector Assessment: ADB Papers on Indonesia," 2015.

[6] INTERNATIONAL FOOD POLICY RESEARCH INSTITUTE, "The Impact of Global Climate Change on the Indonesian Economy," Bogor Agricultural University, IFPRI Discussion Paper 01148 2011.

[7] WORLD BANK, DUKE UNIVERSITY, "Scaling-Up Renewable Geothermal Energy in Indonesia," ESMAP 2014.

[8] ASIAN DEVELOPMENT BANK, THE WORLD BANK, "Unlocking Indonesia's Geothermal Potential," e-ISBN 978-92-9254-902-2, 2015.

[9] MEMR INDONESIA, GEOLOGY DEPARTMENT, "Laporan Akhir Survey Terpadu Geologi dan Geokimia, Daerah Panas Bumi Kepahiang Kabupaten Kepahiang, Provinsi Bengkulu," Bandung, Survey report 2010.

[10] BADAN PUSAT STATISTIK KABUPATEN KEPAHIANG, "Statistik Daerah Kabupaten Kepahiang," yearly report 2016.

[11] MEMR INDONESIA, GEOLOGY DEPARTMENT, "Laporan Akhir Survei Geofisika Terpadu Panas Bumi Daerah Kepahiang, Kabupaten Kepahiang, Provinsi Bengkulu," Bandung, Survey report 2010.

[12] MEMR INDONESIA, GEOLOGY DEPARTMENT, "Laporan Akhir Survey Magnetotelurik Daerah Panas Bumi Kepahiang, Kabupaten, Kepahiang, Bengkulu," Bandung, Survey report 2011.

[13] MEMR INDONESIA, GEOLOGY DEPARTMENT, "Laporan Akhir Survey Landaian Suhu Sumur KPH-1, Daerah Panas Bumi Kepahiang Kabupaten Kepahiang, Provinsi Bengkulu," Bandung, Survey report 2011.

[14] M. ZEYGHAMI and J. NOURALIEE, "Effect of Different Binary Working Fluids on Performance of Combined Flash Binary Cycle," in *Proceedings World Geothermal Congress*, Melbourne, 2015.

[15] R. DIPIPPO, *Geothermal Power Plants*, 4th ed.: Elsevier, 2016.

[16] M.R. KARLSDOTTIR, H. PALSSON, and O.P. PALSSON, "Comparison of Methods for Utilization of Geothermal Brine for Power Production," in *Proceedings World Geothermal Congress* , Bali, 2010.

[17] M. ZEYGHAMI, "Performance analysis and binary working fluid selection of combined flash-binary geothermal cycle," *Energy*, no. 88, pp. 765-774, June 2015.

[18] H., GOSWAMI, D.Y., STEFANAKOS, E.K. CHEN, "A review of thermodynamic cycles and working fluids for the conversion of low-grade heat," *Renewable and Sustainable Energy Reviews*, no. 14, pp. 3059-3067, 2010.

[19] Q., DUAN, Y., YANG, Z. LIU, "Performance analyses of geothermal organic Rankine cycles with selected hydrocarbon working fluids," *Energy*, no. 63, pp. 123-132, November 2013.

[20] CALIFORNIA ENERGY COMMISSION (CEC), "Estimated Cost of New Renewable and Fossil Generation in California," Staff 2014.

[21] A., BOLATTURK, A., KONOGLU, M. COSKUN, "Thermodynamic and economic analysis and optimization of power cycles for a medium temperature geothermal resource," *Energy Conversion and Management*, no. 78, pp. 39-49, 2014.

[22] GEOTHERMAL ENERGY ASSOCIATION, "Factors Affecting Costs of Geothermal Power Development," U.S. Department of Energy 2005.

[23] U.S. ENERGY INFORMATION ADMINISTRATION (EIA), "Updated Capital Cost Estimates for Utility Scale Electricity Generating Plants," 2013.

[24] V. STEFANSSON, "Investment cost for geothermal power plants," in *Proceeding of the 5th Inaga Annual Scientific Conference & Exhibitions*, Yogyakarta, 2001.

[25] A., KRISTIANTO A.W., A. SUGIANTO, "Survey Magnetotellurik Daerah Panas Bumi Kepahiang, Kabupaten Kepahiang, Bengkulu," Prosiding Hasil Kegiatan Pusat Sumber Daya Geologi 2011.